What can GLAST tell us about AGNs?

Chuck Dermer **(Naval Research Laboratory)**

GLAST LAT Collaboration Meeting, October 24, 2002

Outline

Introduction: GLAST and AGNs

1. **Radio-Quiet and Radio-Loud AGNs**
2. **Blazars**

Leptonic Models

1. **Radiation Processes**
2. **Electron Injection and Energy Losses**
3. **What GLAST observations mean for blazar properties, e.g., B-field and Doppler factor δ**

Hadronic Models

1. **Photomeson Production**
2. **Neutrino and Gamma-Ray Production**
3. **Neutral Beam Formation**

Extended Jets

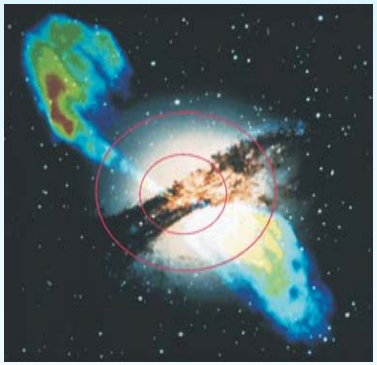

Cen A

Misaligned blazars

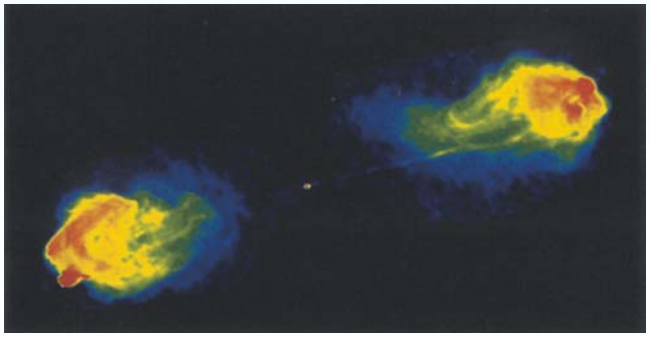

Cyg A

Sensitivity of GLAST for High Latitude AGN Detection

On-Axis Effective Area $$A = 6200\,(\frac{E}{E_{100}})^{0.16}\ cm^{-2}$$

Source νF_ν Flux $$\nu F_\nu = 10^{-10} f_{-10}\,(\frac{E}{E_{100}})^{\alpha_\nu}\ ergs\ cm^{-2}\ s^{-1}$$

Source Counts $$S \approx 19\ Xt_4 f_{-10}\,(\frac{E}{E_{100}})^{-1.84+\alpha_\nu} \quad (>1)$$

Diffuse Extragalactic Background Counts
(Acceptance cone = psf) $$B \approx 12\ Xt_4\,(\frac{E}{E_{100}})^{-2.27}$$

$$\frac{S}{\sqrt{B}} \approx 5\sqrt{Xt_4}\, f_{-10}\,(\frac{E}{E_{100}})^{\alpha_\nu - 0.71} \quad (>3-5)$$

Radio-Quiet AGN: Seyferts AGNs and QSOs

Radio Quiet: F(5 GHz)/F(B Band) < 10

- Sy 1: broad (~2000-20000 km/s) permitted optical/UV lines; narrow (~500 km/s) permitted and forbidden lines
- Sy 2: narrow permitted and forbidden lines
- **QSOs:** scaled-up Seyferts (dividing line at 10^{45} ergs/s)

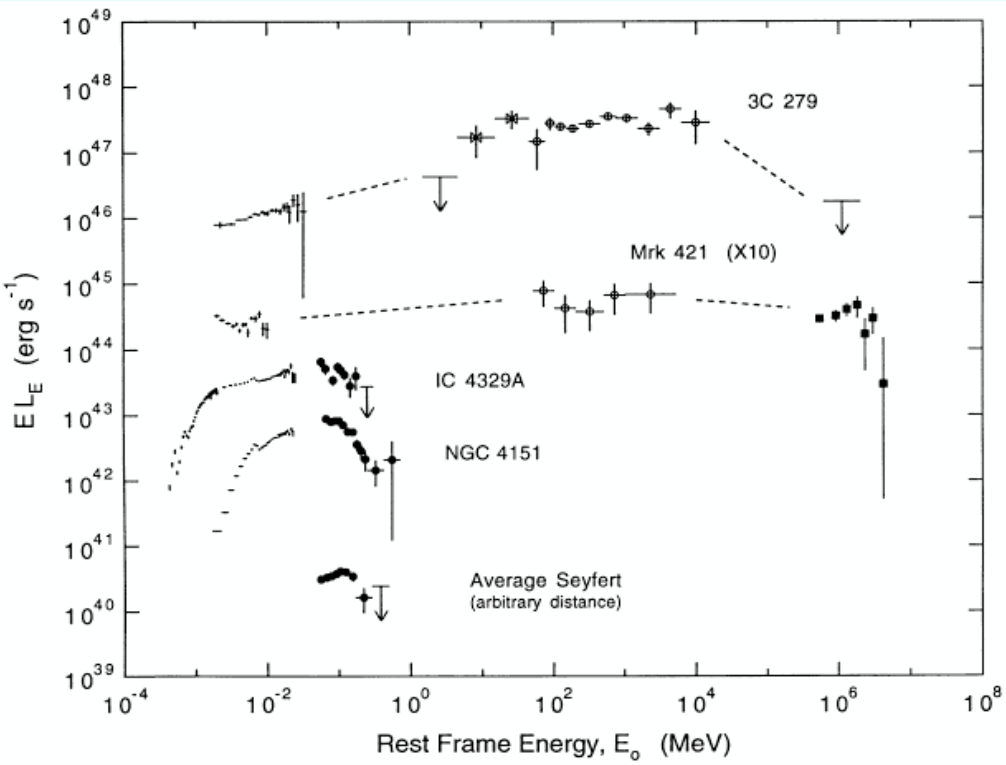

AGN *Cartoon*

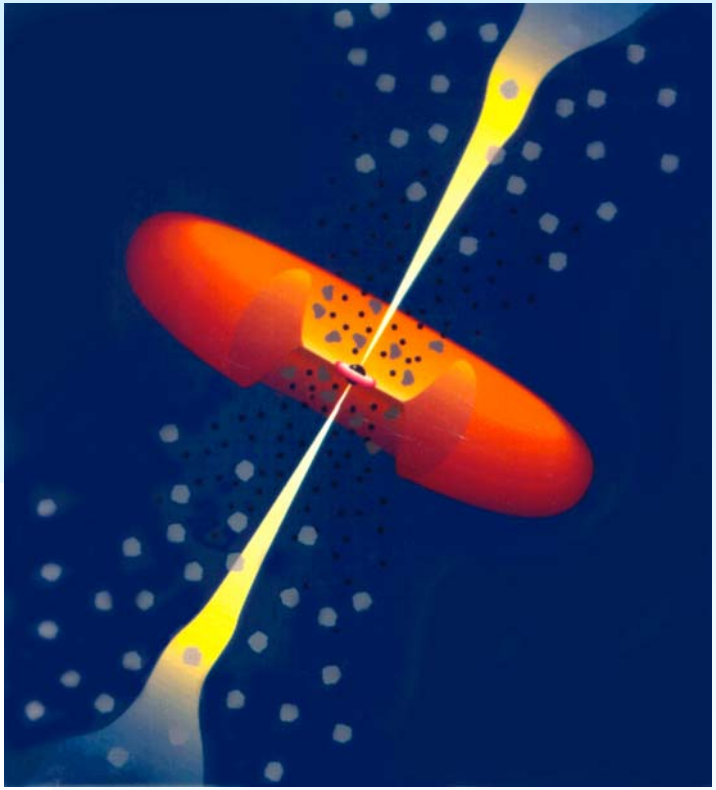

Host Galaxies Types:
Spirals and Ellipticals

No evidence for >> MeV emission in radio-quiet AGNs

Radio (Loud) Galaxies

Fanaroff-Riley (1974) Classification Scheme

- FR I: separation between the points of peak intensity in the two lobes is smaller than half the largest size of the source
  - Edge-darkened, twin jet sources
- FR II: separation between the points of peak intensity in the two lobes is greater than half the largest size of the source.
  - Edge-brightened hot spots and radio lobes, classical doubles

Morphology correlates strongly with radio power at 2×10^{25} W/Hz at 178 MHz ($\cong 4 \times 10^{40}$ ergs s^{-1}), or total radio power of $\cong 10^{42}$ ergs s^{-1}

Optical emission lines in FR IIs brighter by an order of magnitude than in FR Is for same galaxy (elliptical or disturbed) host brightness

FR I: low luminosity, twin jet sources

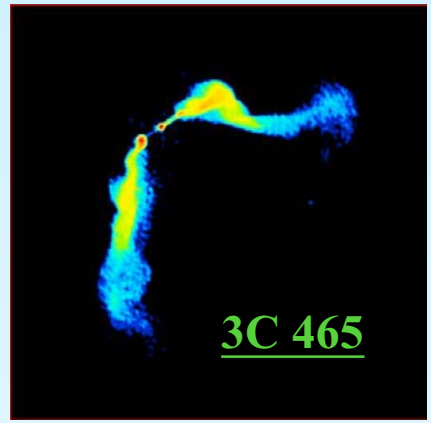

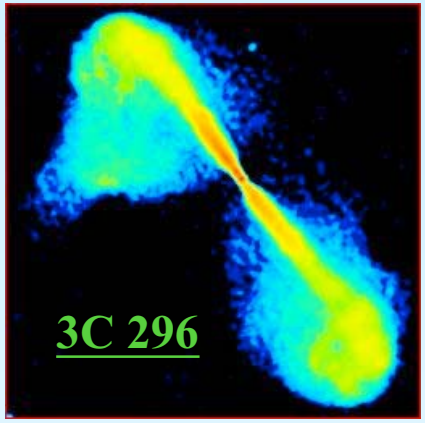

FR II: high luminosity, lobe dominated

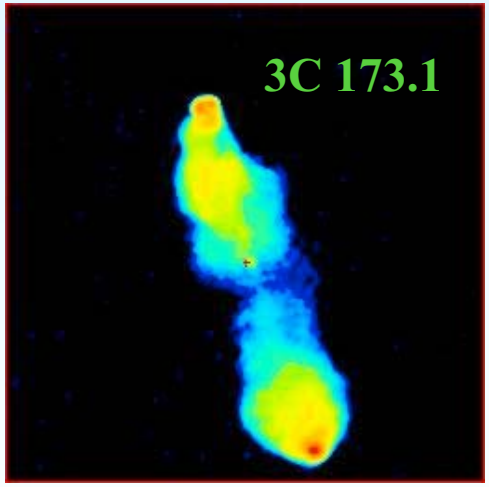

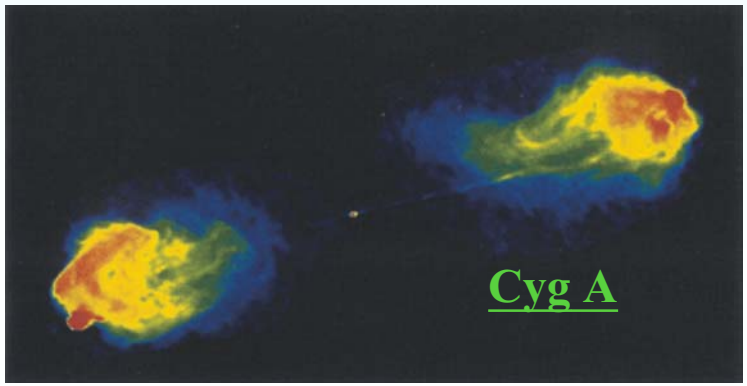

Blazars

Class of AGNs which includes optically violently variable quasars; highly polarized quasars, flat spectrum radio sources, superluminal sources

- BL Lac objects – nearly lineless (equivalent widths < 5 Å: ⇒ dilute surrounding gas)
- Flat Spectrum Radio Quasars (strong emission lines: ⇒ dense broad line region clouds)

Blazars: radio galaxies where jet is pointed towards us; radio galaxies = misaligned blazars

FR Is are parent population of BL Lac objects; FR IIs are parent population of FSRQs

(Urry and Padovani 1995)

$L \sim 10^{45} \times (f/10^{-10}$ ergs cm^{-2} s^{-1}) ergs s^{-1}

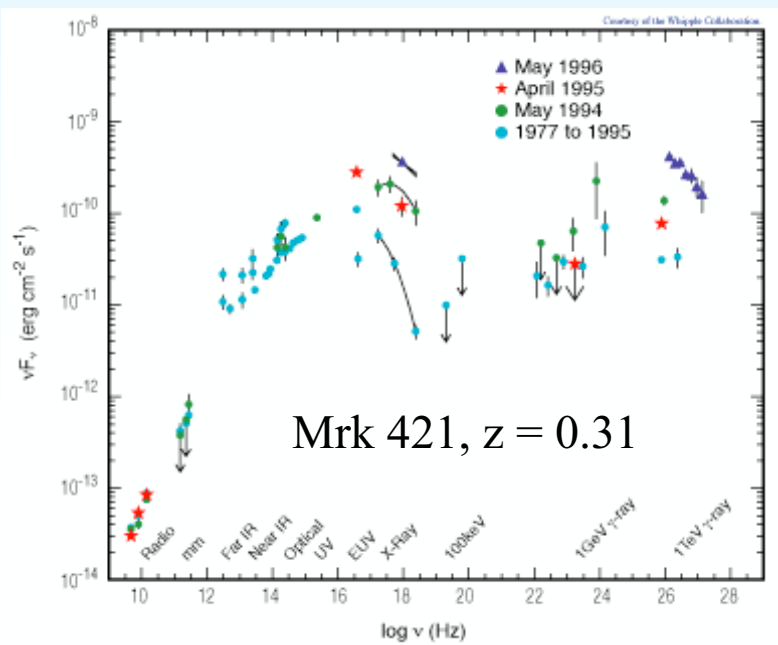

$L \sim 5 \times 10^{48} \times (f/10^{-9}$ ergs cm^{-2} s^{-1}) ergs s^{-1}

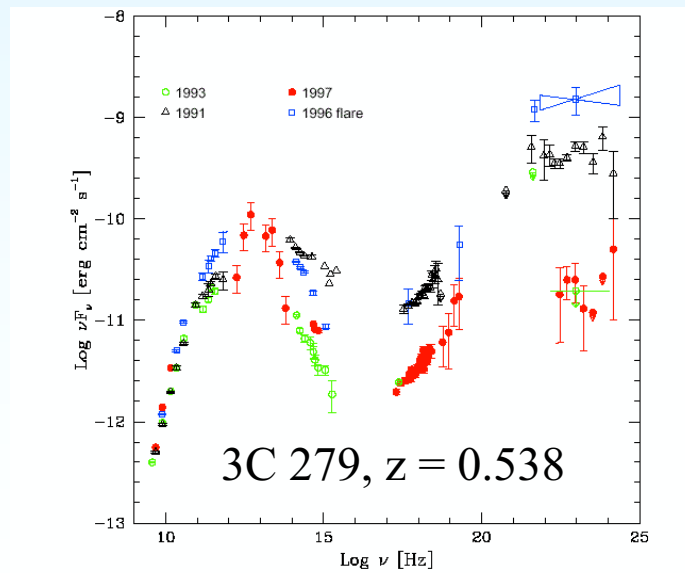

Figure 2. Quasi-simultaneous SEDs of the quasar 3C279 taken in the different epochs. The *Beppo*SAX and EGRET data taken in 1997 are almost exactly contemporaneous, while the ISO spectrum is taken one month before.

Transitional Types: 3C 273

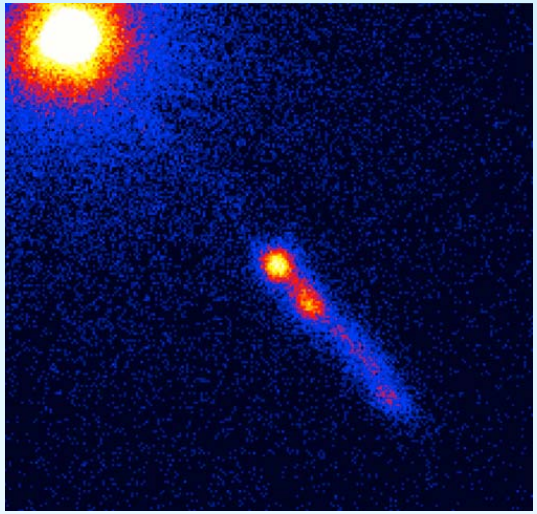

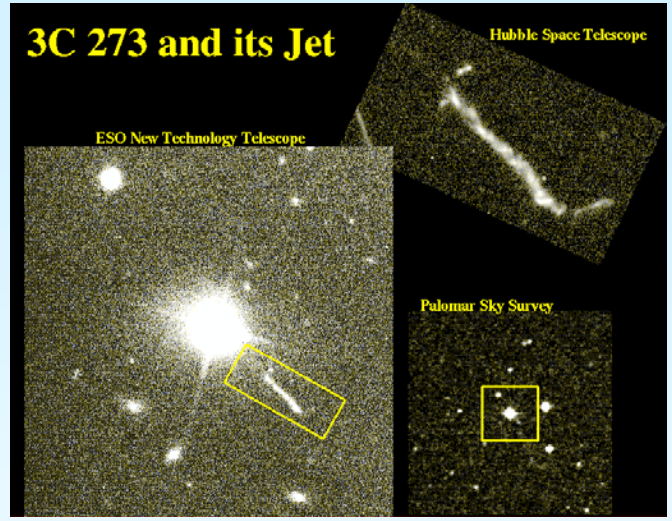

Observations of the jet of 3C 273 with Chandra (left, Sambruna et al. 2001), and at other frequencies (right)

Nucleus, Hot Spots, Lobes

$z = 0.158$

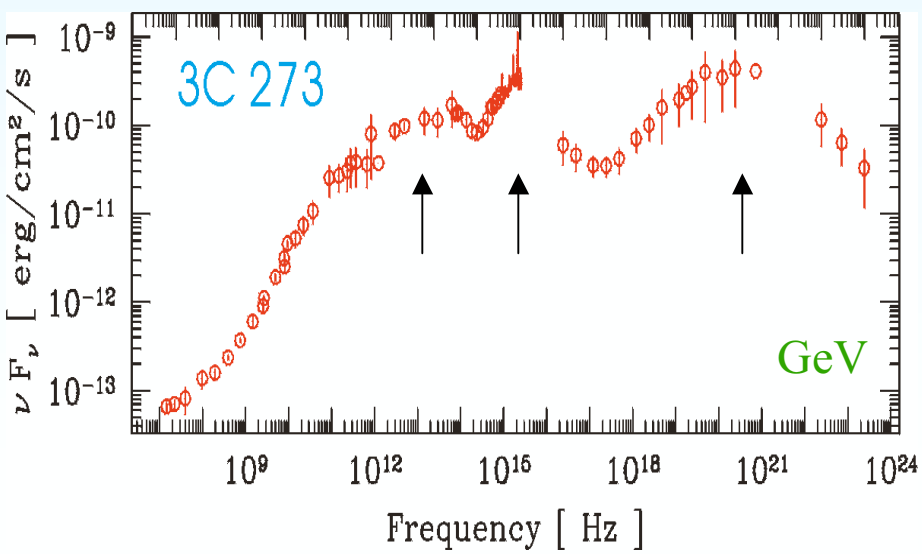

Sllightly misaligned blazar

Blazar 3C 279

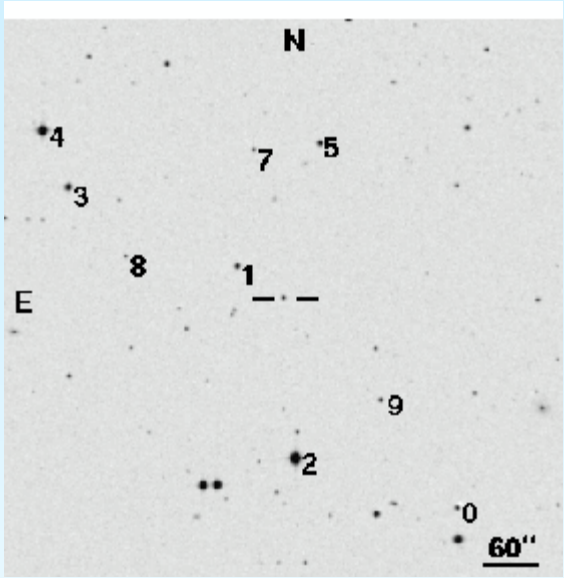

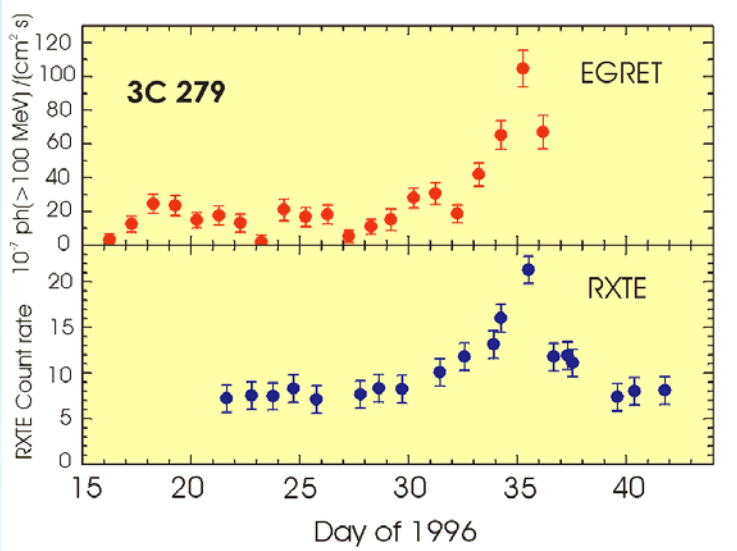

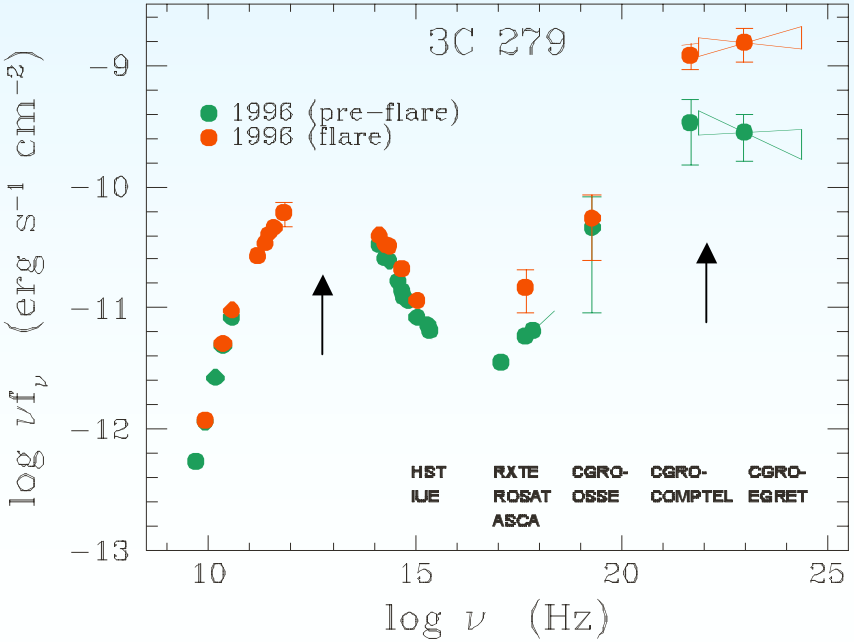

$z = 0.538$, $d_L = 8.8\times10^{27}$ cm

Gamma-ray luminosity:
$\sim 5\times10^{48}\ f_B$ ergs s^{-1}

Variability timescale at gamma-ray energies:

$dL/dt \sim 6\times10^{43}$ erg / s^2

"energy acceleration"

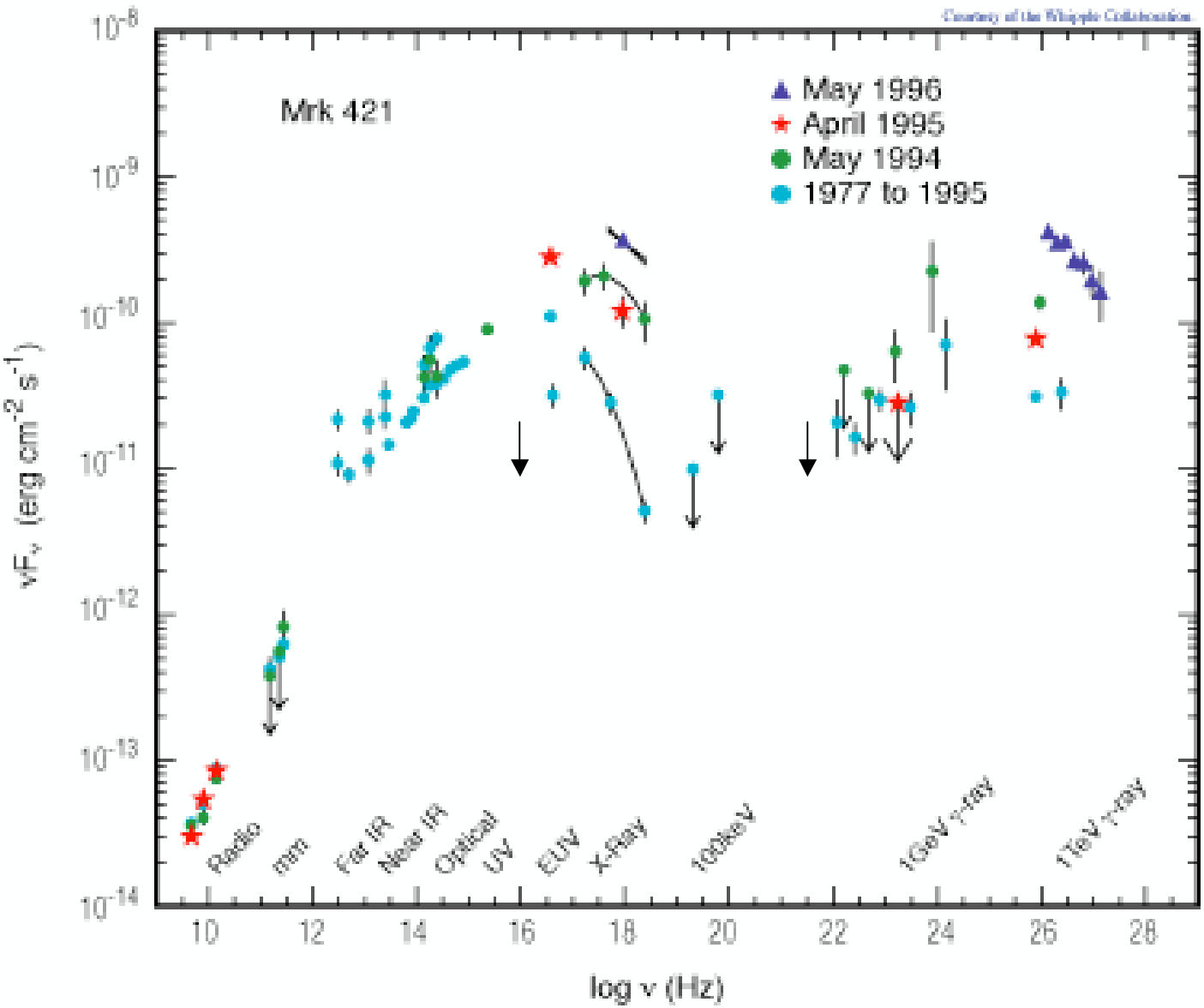

Macomb et al. 1996

HBL Lac: Mrk 421

$z = 0.031$

$d_L = 4.4 \times 10^{26}$ cm

Apparent isotropic gamma-ray luminosity: $\sim 10^{45}$ f_{-10} ergs s^{-1}

Variability timescale at TeV energies: ~ 15 min

HBL Mrk 501

$z = 0.033$

$d_L \approx 150$ Mpc

Gamma-ray luminosity:
$\sim 10^{45}\ f_{-10}$ ergs s^{-1}

Variability timescale at TeV energies: < 1 day

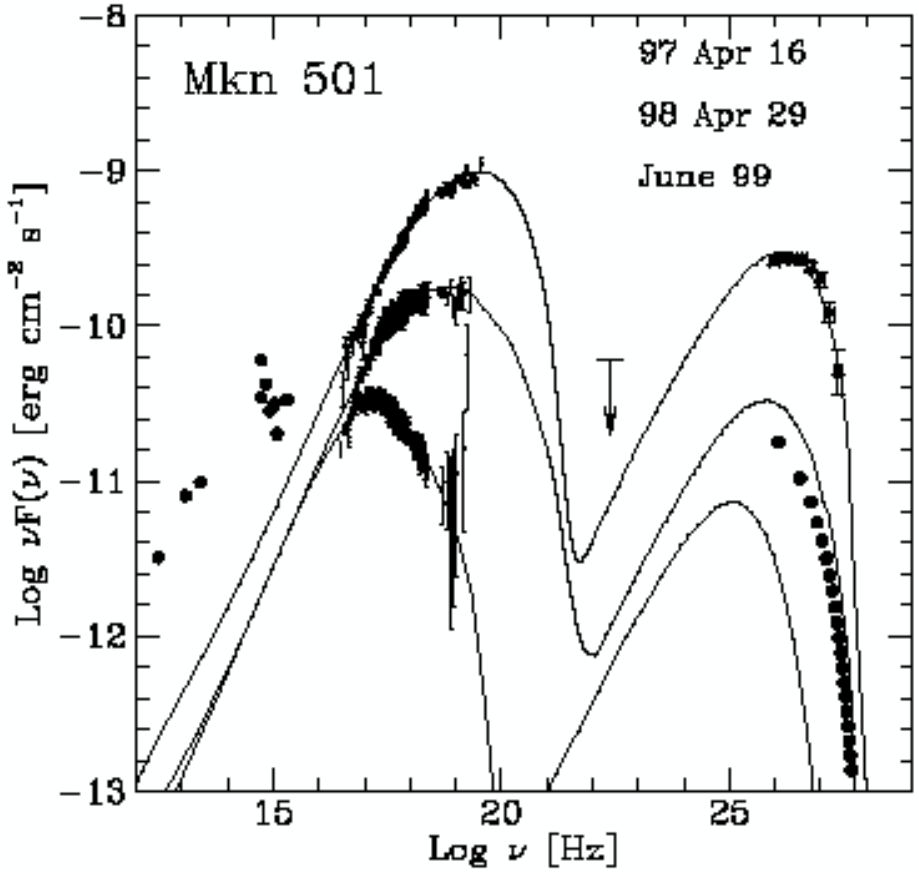

FIG. 7.—Overall SED of Mrk 501 of 1997 April 16, 1998 April 29, and 1999 June. The solid line is the spectrum calculated with the homogeneous SSC model described in the text. The filled circles are from the HEGRA 1998–1999 data (from Aharonian et al. 2001).

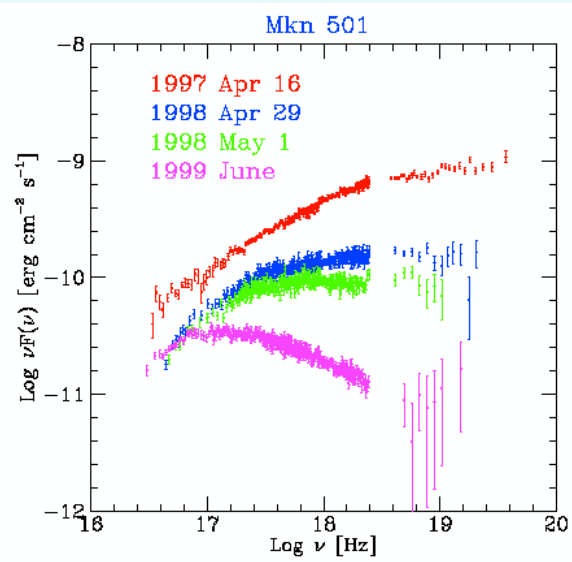

Maraschi and Tavecchio 2001

Blazar SED Sequence

Finding an order in the SEDs of blazars

E_{pk} of synchrotron and Compton components inversely correlated with L

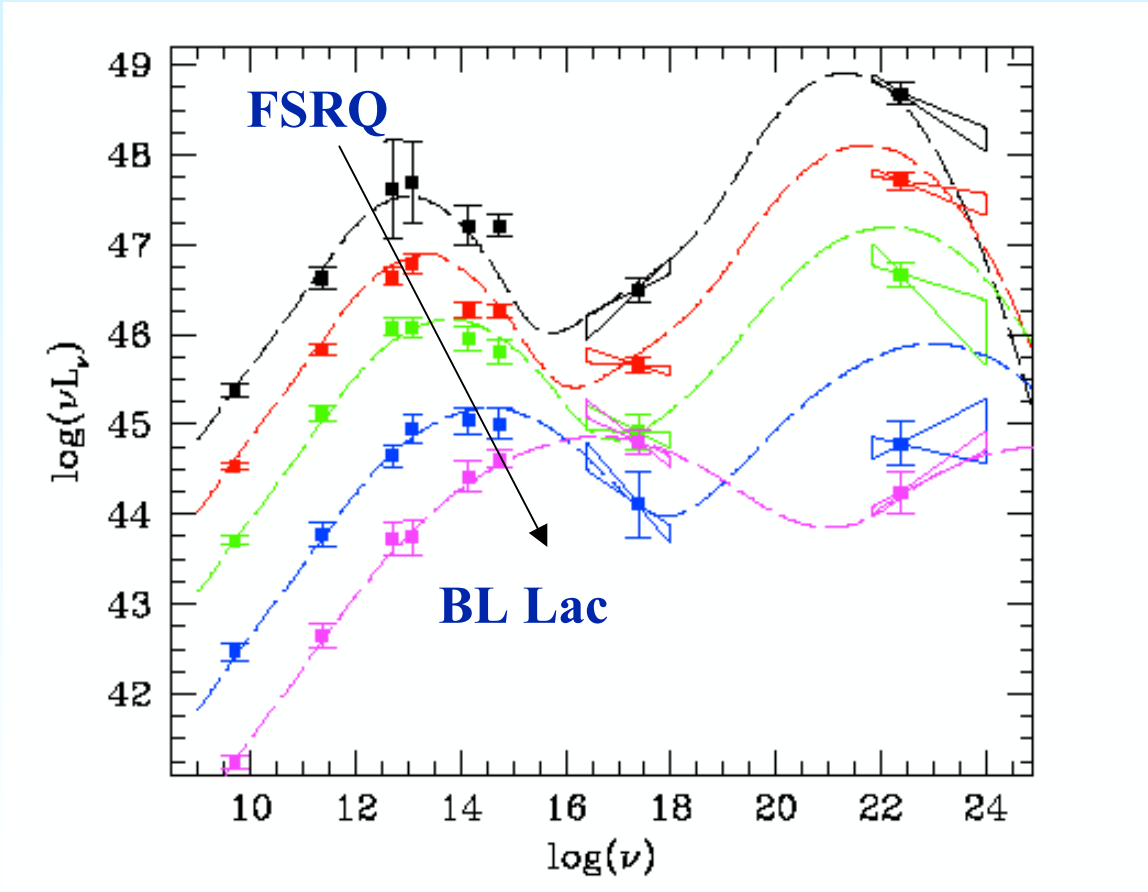

Sambruna et al. 1996; Fossati et al. 1998

Redshift and Luminosity Distribution of Gamma Ray Blazars

Redshift (left) and luminosity (right) distribution of 60 high confidence gamma-ray blazars (14 BL Lac objects and 46 FSRQs) in the Third EGRET catalog (Hartman et al. 1999).

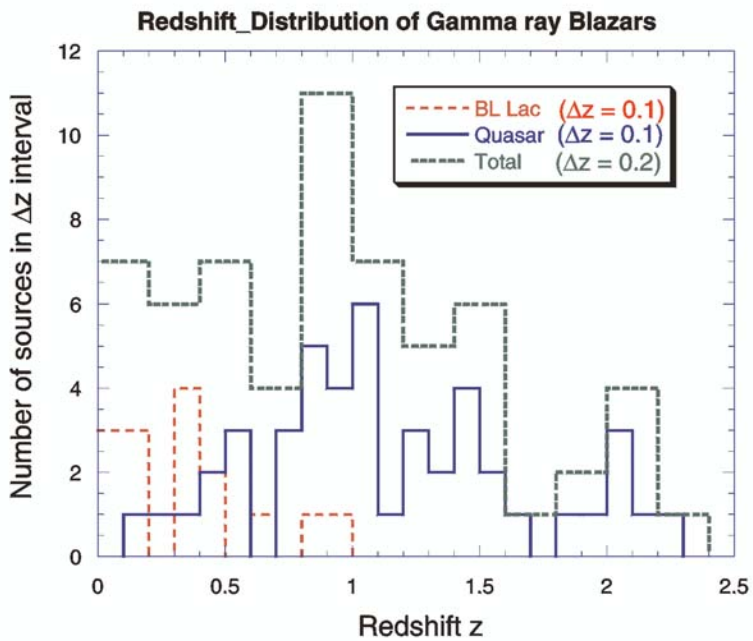

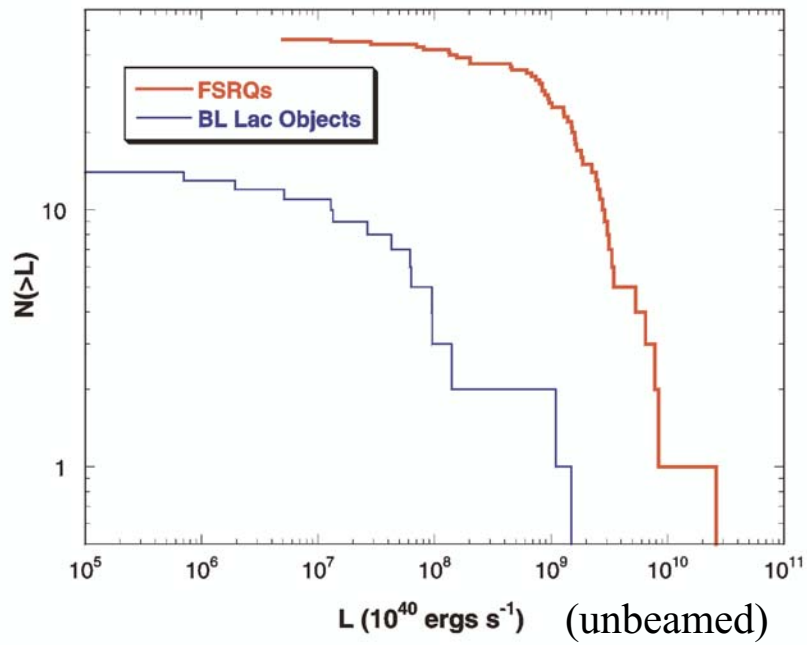

(unbeamed)

(Not including sources within 10° of the Galactic plane.) Catalogs of Padovani & Giommi (1995) and Perlman et al. (1996) used for BL Lac idenitfications.

- BL Lacs: less numerous and closer, with an average redshift of ~ 0.5
- FSRQs: average redshift peaks at z ~ 1, with tail reaching to z ~ 2.3.
- Luminosities of FSRQs are 1-2 orders of magnitude greater than those of the BL Lacs
- Thousands of blazars and tens of radio galaxies with GLAST -- depending on population evolution and luminosity functions

Gamma Ray Blazar Spectral Indices

> 100 MeV peak spectral indices from Third EGRET catalog

No evidence for K-correction

Insufficient statistics to examine > 1 GeV spectral indices

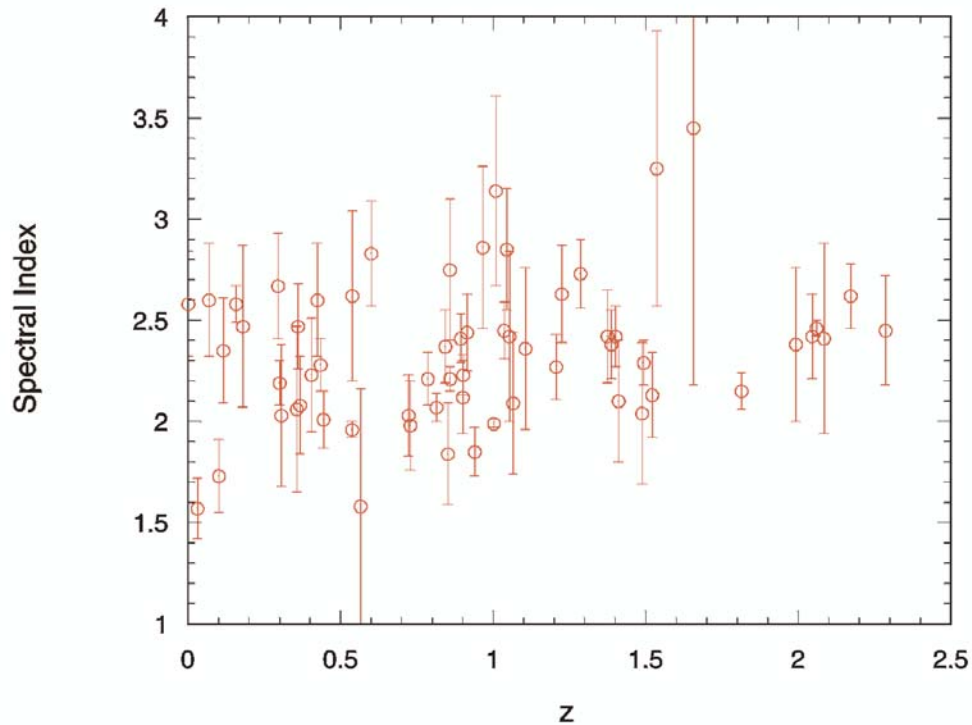

GLAST sensitivity can examine > 1 GeV spectral indices and spectral cutoffs from:

- Intrinsic cutoffs of radiating sources
- $\gamma\gamma$ opacity due to local radiation fields
- $\gamma\gamma$ opacity due to cosmic diffuse radiation fields

Black Hole/Accretion Disk/Jet Physics

Jet origin: Poynting flux (Blandford-Znajek process), pair outflow, exhaust gas -- composition of jet

Jet collimation: magnetic vs. hydrodynamic

Inner jet models: Accelerating vs. decelerating jet models

Disk-jet symbiosis (galactic microquasar studies): Relationship of jet power to disk power (Falcke et al.)

Reverberation mapping: GLAST may discover imprint of disk radiation in attenuated GeV emission (Böttcher and Dermer 1995)

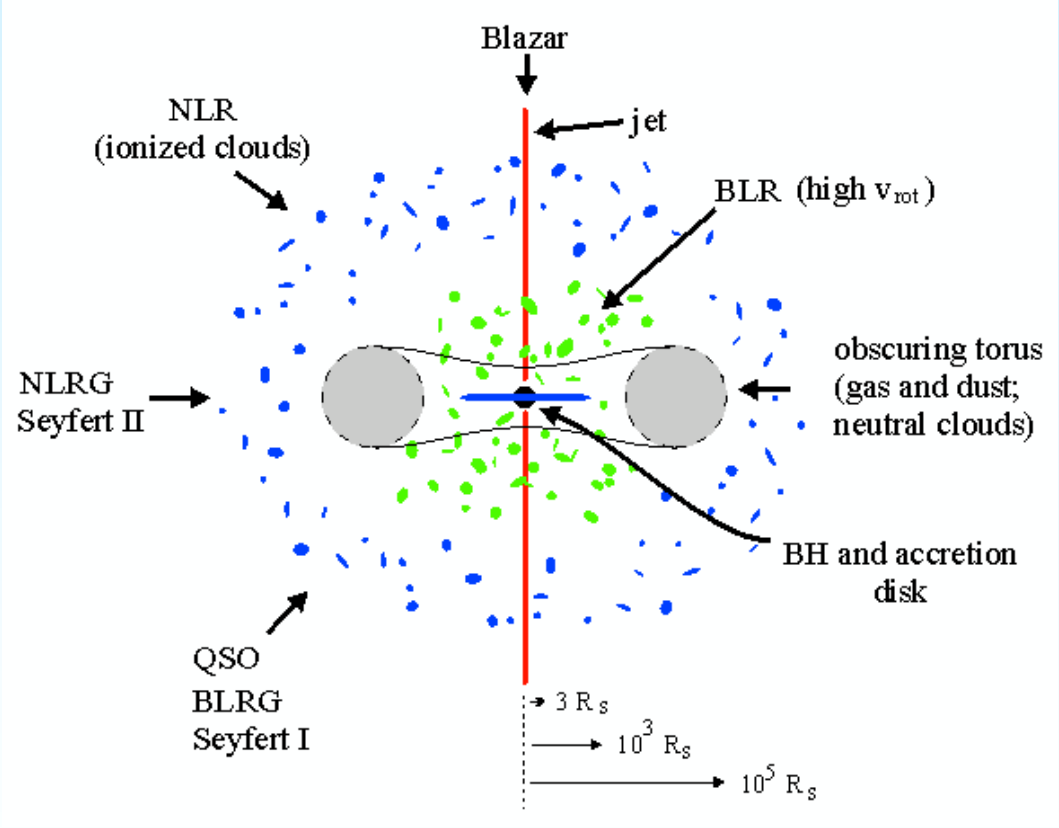

Reverberation Mapping of the AGN Environment

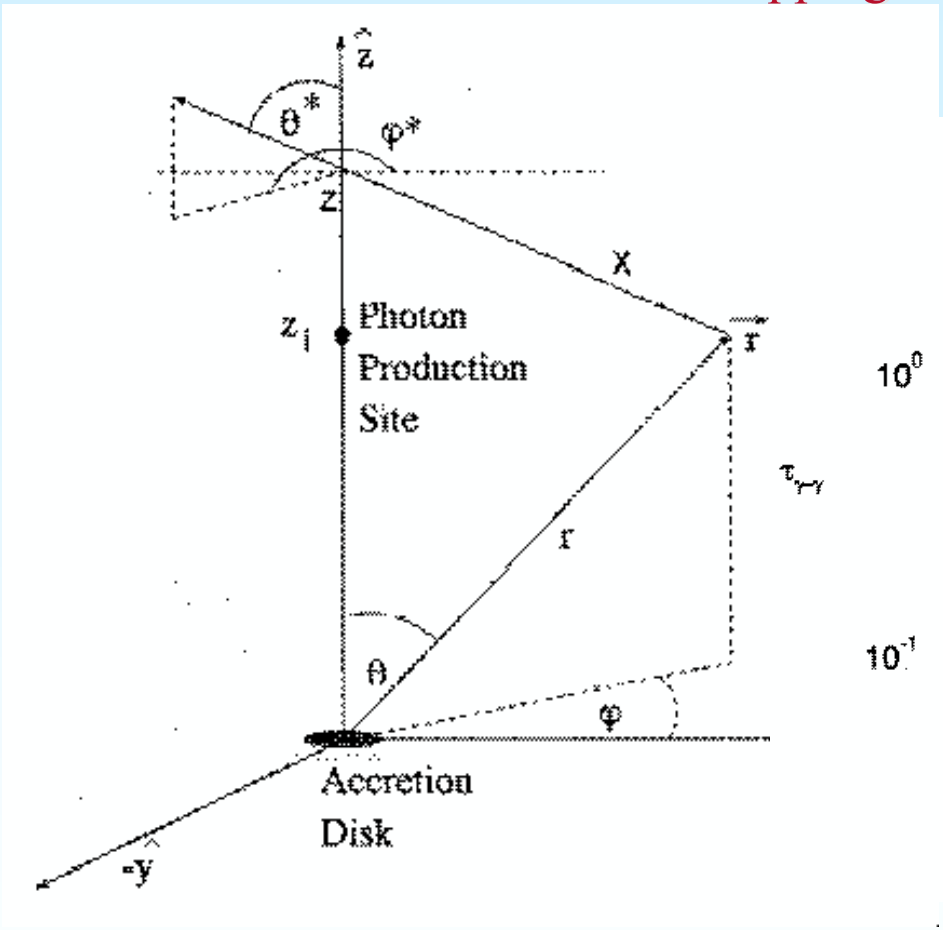

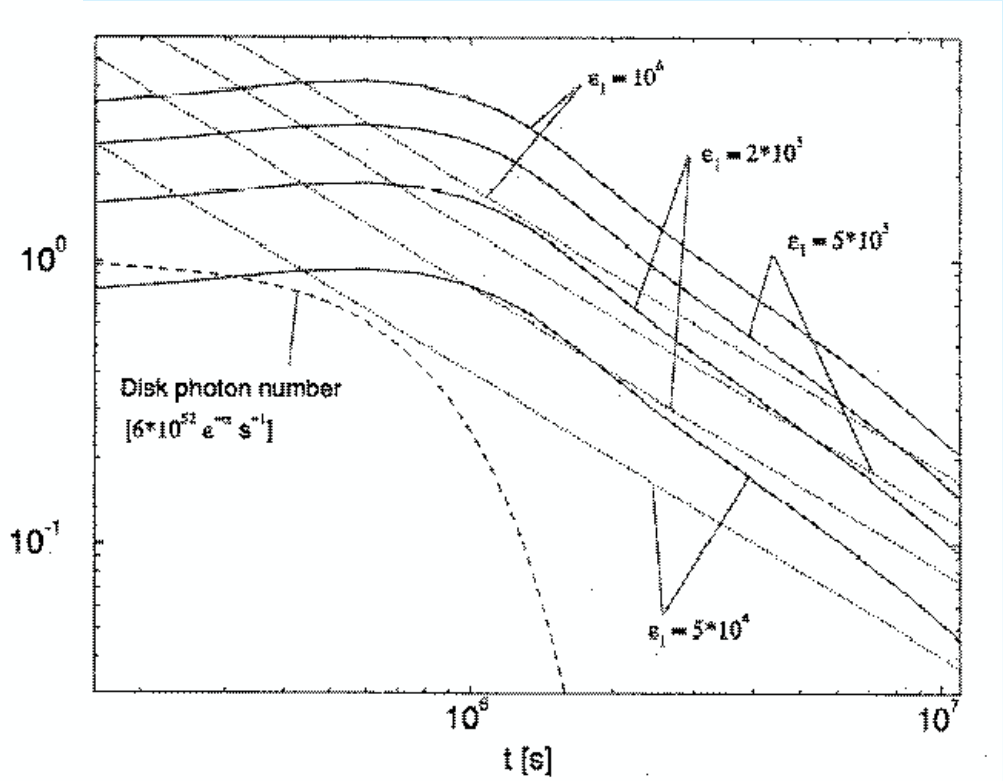

- Anti-correlation with Broad Emission Lines (or Big Blue Bump) and Cutoff

Evidence for Relativistic Outflows

1. Synchrotron Self-Compton Limits

(aka Compton catastrophe)
Observe L_{radio}, ν_{radio}, Δt or $\Delta\theta \Rightarrow$ radius R, u_{syn}

Synchrotron self-absorption frequency $\Rightarrow$ B from synchro-Compton theory

Ratio $u_{syn} / (B^2/8\pi) >> 1 \Rightarrow$ large flux of synchrotron self-Compton X-rays (not seen)

Resolution:

Beaming (Woltjer 1966) or
Bulk relativistic motion (Blandford and Rees 1978)

Provides information on bulk outflow at the 0.1-1 pc scale where radio emission is formed (gravitational radius is 10^{-4} pc for 10^9 Solar mass black hole)

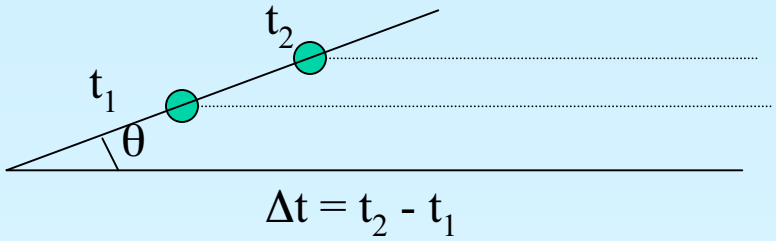

2. Apparent Superluminal Motion

$\Delta t_{obs} = \Delta t(1-\beta\cos\theta)$

$\Delta x_{\perp} = \beta c \Delta t \sin\theta$

$\Rightarrow \beta_{\perp} c = \Delta x_{\perp} / \Delta t_{obs} = \beta c \sin\theta/(1-\beta\cos\theta)$

$\rightarrow \quad \beta \Gamma c$

$(\Gamma >> 1, \theta \approx 1/\Gamma)$

Apparent SL motion now seen from scores of radio sources, with apparent SL speeds typically between 1 and 10, though with a few reaching ~ 20 (Vermeulen and Cohen 1994)

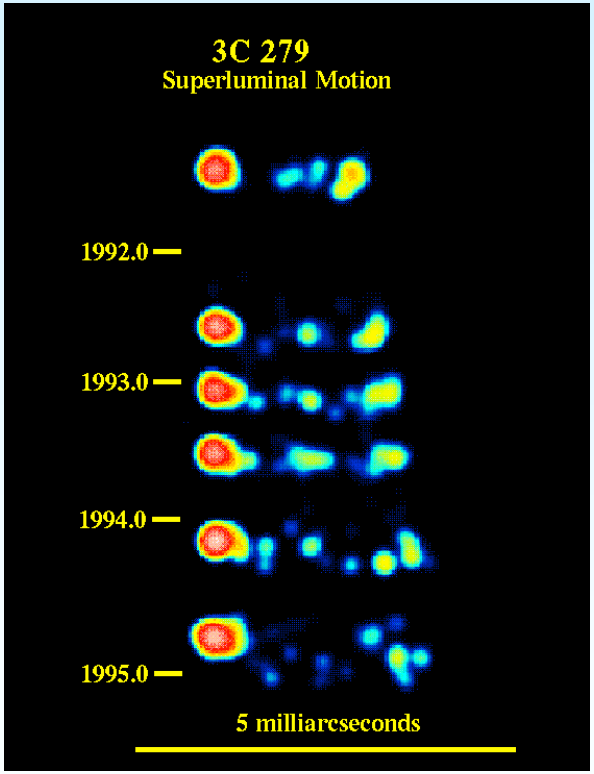

Again, provides information on bulk outflow at the 0.1-1 pc scale where radio emission is formed.

3. γγ Transparency Arguments

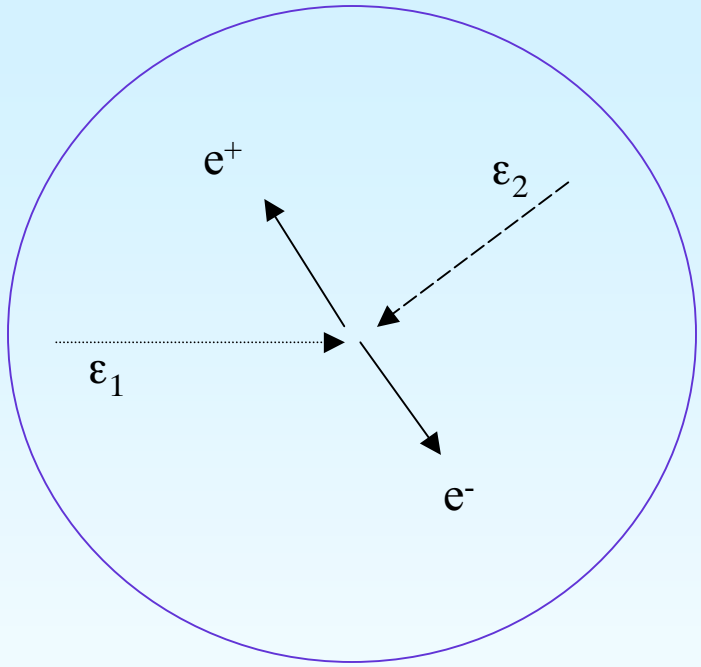

Threshold condition

$$s = \varepsilon_1\, \varepsilon_2 = E_1\, E_2 /(m_e c^2)^2 > 1$$

Cross section $\sigma_{\gamma\gamma} \approx \sigma_T / s$

For γ-ray transparency ($\varepsilon_1 = \varepsilon_\gamma$)

$$n_2\, \sigma_{\gamma\gamma}\, R < 1$$

$R \sim c\, \Delta t_{1,2}$ (correlated observations or cospatial assumption)

$n_2 \sim L_2/[E_2(4\pi R^2 c)] \Rightarrow$

$$\frac{L_2}{[E_2(4\pi R^2 c)]}\, \frac{\sigma_T}{\varepsilon_1\, \varepsilon_2} < 1$$

$$\Rightarrow \frac{L_2}{\Delta t_{1,2}} < \frac{(4\pi c^2 \varepsilon_1\, \varepsilon_2)\, E_2}{\sigma_T}\ , \quad \varepsilon_1\, \varepsilon_2 < 1$$

$\varepsilon_1 \rightarrow \varepsilon_\gamma$, $\varepsilon_2 \rightarrow \varepsilon_X$, $\varepsilon_\gamma\, \varepsilon_X \sim 1 \Rightarrow$

$$\frac{L_X}{\Delta t_{X,\gamma}} < \frac{4\pi c^2\, E_X}{\sigma_T}$$

Probe of site of gamma-ray production (within 10^2-10^4 Rs of supermassive black hole)

4. Elliot-Shapiro Relation

Assume stationary emission region

$L_{Edd} = 1.26 \times 10^{46}\ M_8$ ergs s^{-1}

$\Delta t > Rs/c \approx 3 \times 10^{13}\ M_8 / c \approx 10^3\ M_8$ s

$\therefore\ L/\Delta t < 10^{43}\ k_C$ ergs s^{-2} ; k_C corrects for Klein-Nishina effects

(Dermer and Gehrels 1995)

5. Other tests

(Catanese et al. 1997)

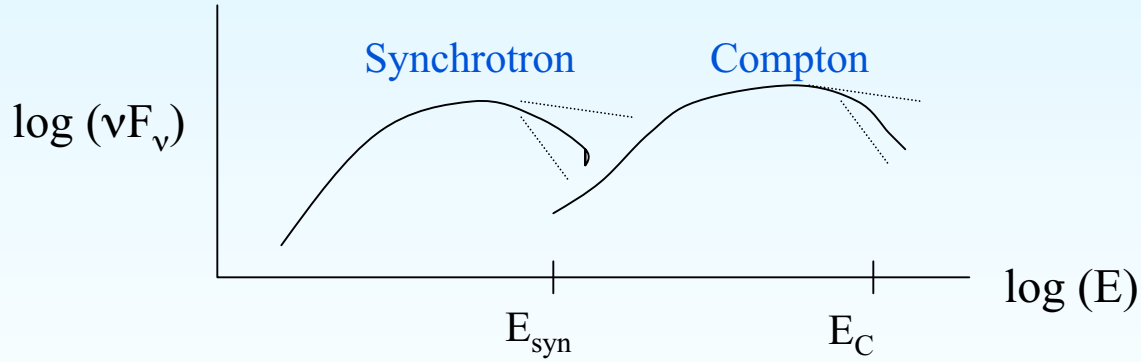

Correlated variability between optical/X-ray and GeV/TeV

1. Observation of synchrotron and Compton cutoffs $\Rightarrow B \approx 2E_{syn}(eV)\ \delta / [E_C(GeV)]^2$
2. Variability of synchrotron component (assumed due only to synchrotron radiation) $\Rightarrow B_{min}$

$$\Rightarrow [E_{syn}(eV)\ \delta\ \Delta t(day)]^{-1/3} < B(Gauss) < 2E_{syn}(eV)\ \delta / [E_C(GeV)]^2$$

Violation $\Rightarrow$ beaming

Variability Studies of Blazars with GLAST

Using beaming tests, GLAST observations can chart the variation of Doppler factor with time; test accelerating and decelerating jet models

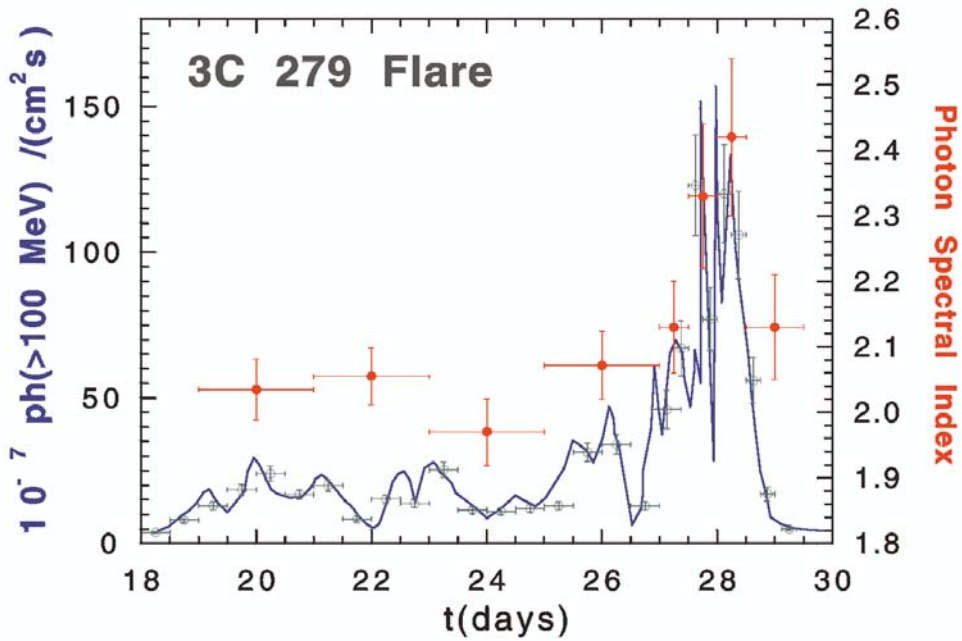

- Spectral index/flux behavior
- E_{pk}/flux behavior
- Spectral index/E_{pk} behavior

Important to probe correlated γ/X behavior

Particle Radiation and Acceleration Processes in Blazar Jets

Standard Blazar Model:

• collimated ejection of plasma with small baryon loading (i.e., bulk Lorentz factor $\Gamma >> 1$)

• reconversion of directed outflow kinetic energy through internal or external shocks

• particle acceleration and radiation

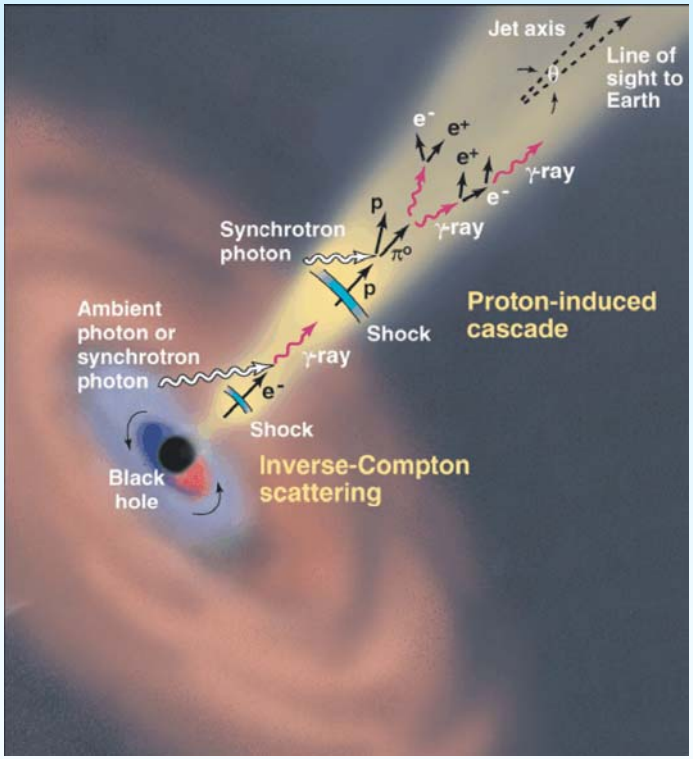

(courtesy J. H. Buckley)

Radiation:

• peaks in SED: nonthermal synchrotron and Compton (SSC, external Compton, reflected Compton) components, blue bump, dust component

Beaming pattern:

• synchrotron and SSC. Flux density $F \propto \delta^{3+\alpha}$

• external Compton. $F \propto \delta^{4+2\alpha}$

$\delta = 1/[\Gamma(1-\beta\cos\theta)]$ is Doppler factor

Radiating Particles:

• primary electrons

• secondary leptons from hadrons which form cascade through photomeson, photopair, and proton synchrotron emission

Standard Blazar Model

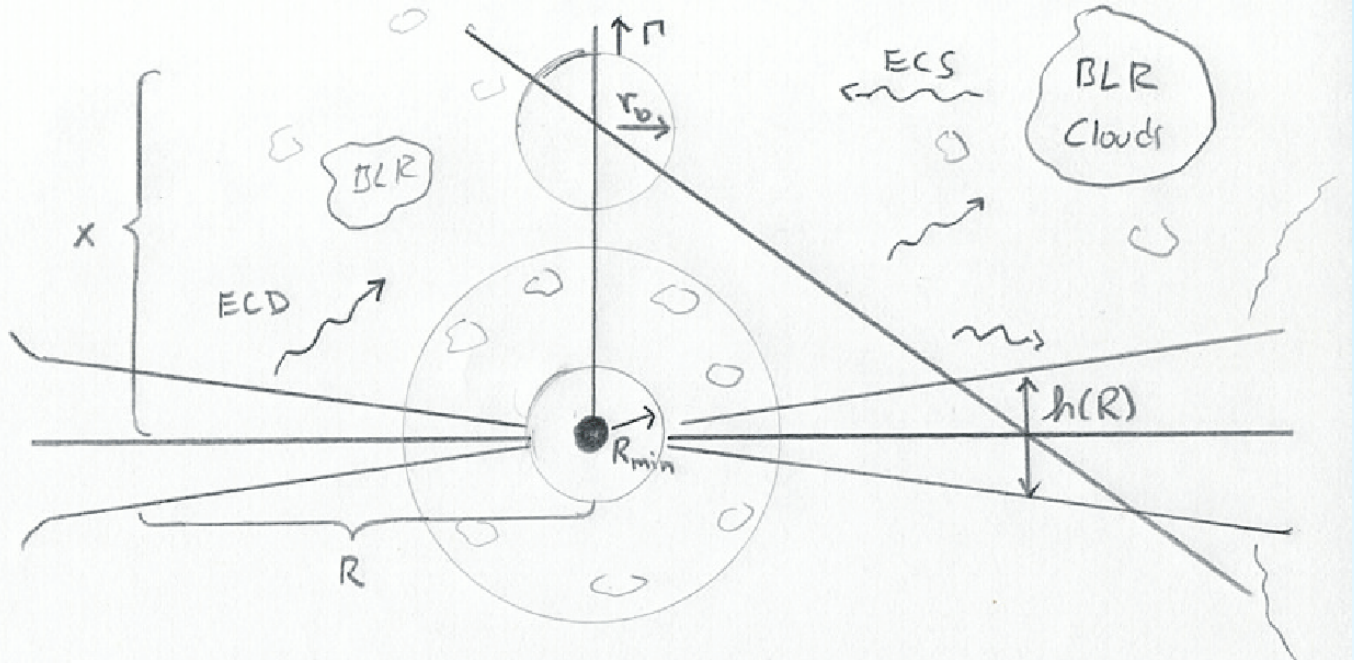

Nonthermal electron synchrotron and Compton processes

Various sources of soft photons:
- disk photons
- disk radiation scattered by BLR
- reflected synchrotron radiation
- radiation from ion torus, etc.

Multiwavelength Blazar Spectra

Leptonic processes: Nonthermal synchrotron radiation

Synchrotron self-Compton radiation,

Accretion disk radiation

Disk radiation scattered by broad-line clouds

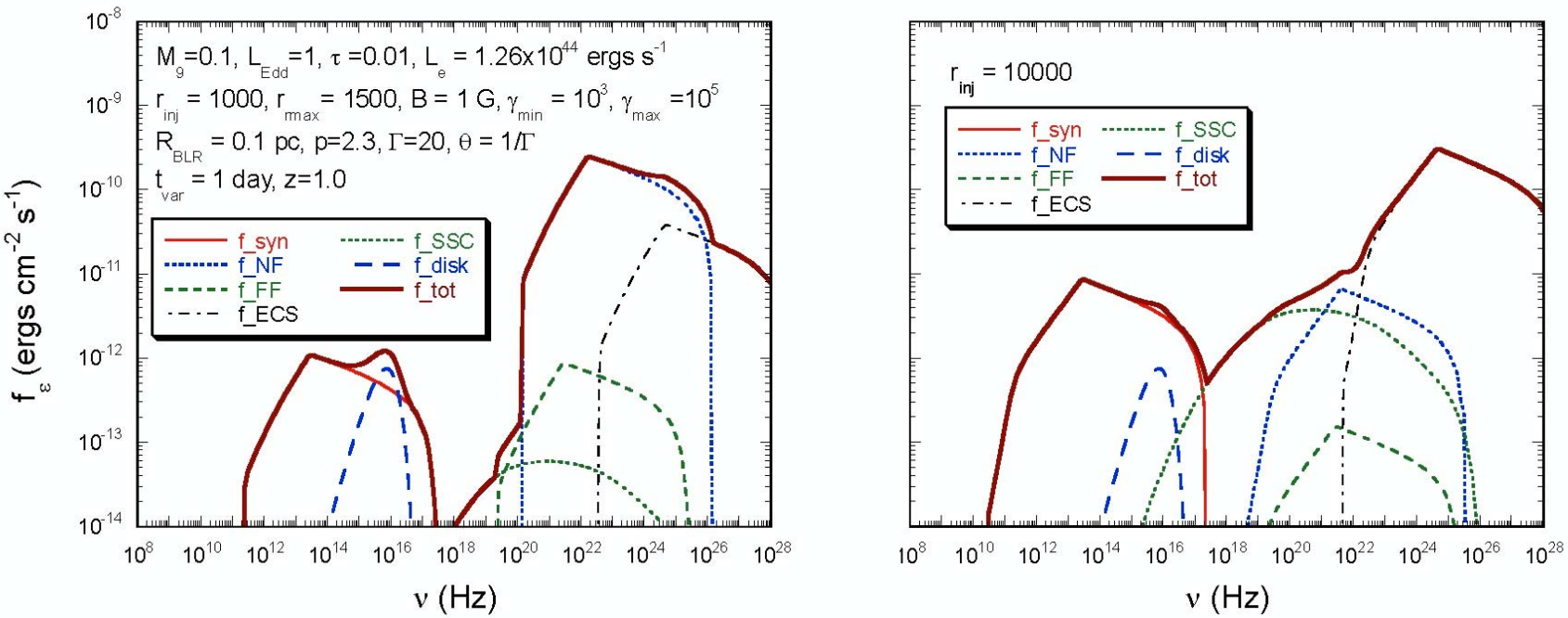

CD and Schlickeiser (2002)

Blazar Variability

Location of gamma-ray production site can be measured with GLAST

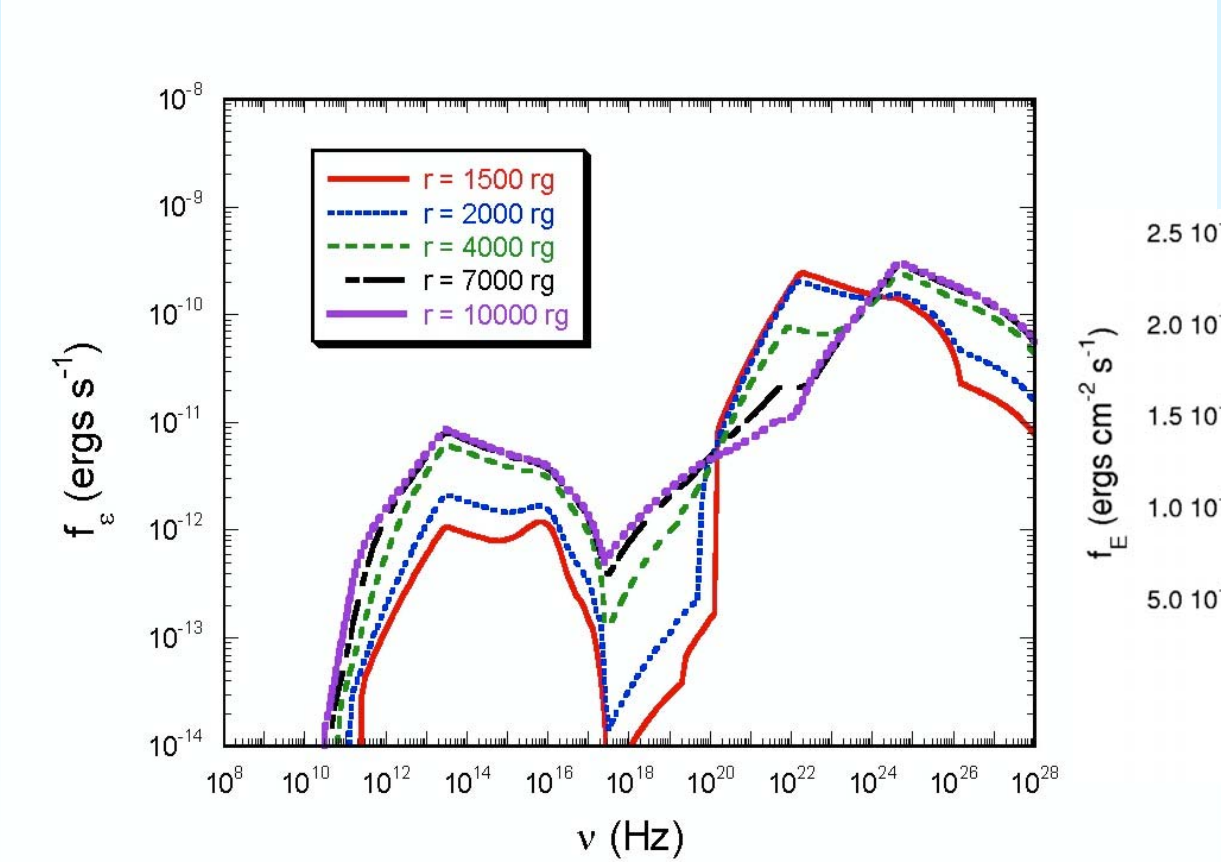

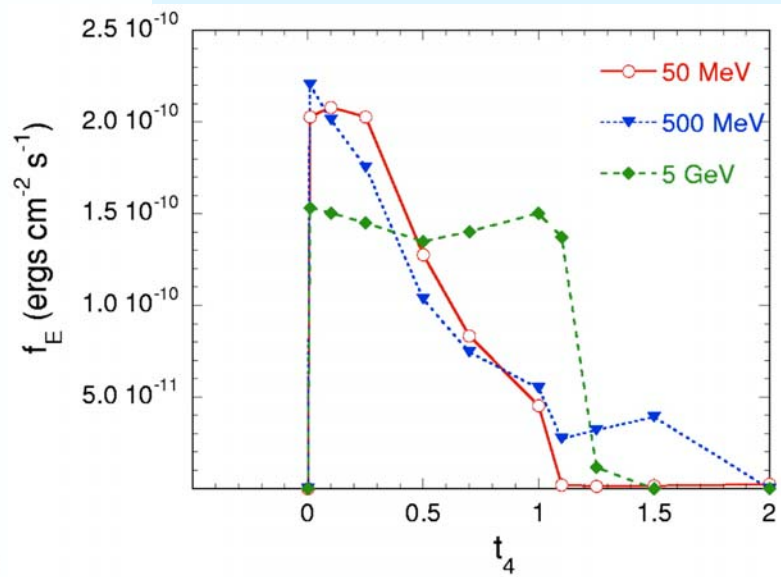

Characteristic variability pattern if disk component important

Spectral Modeling

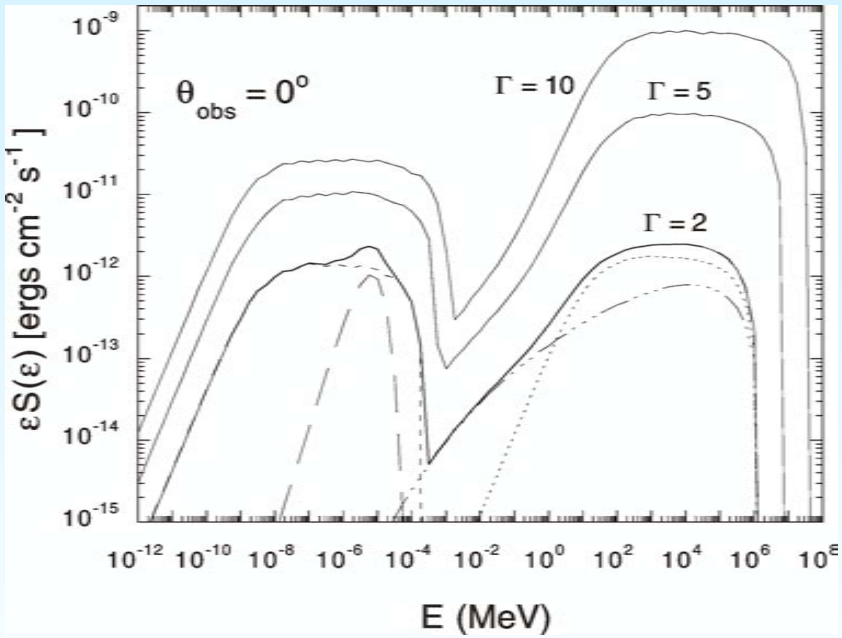

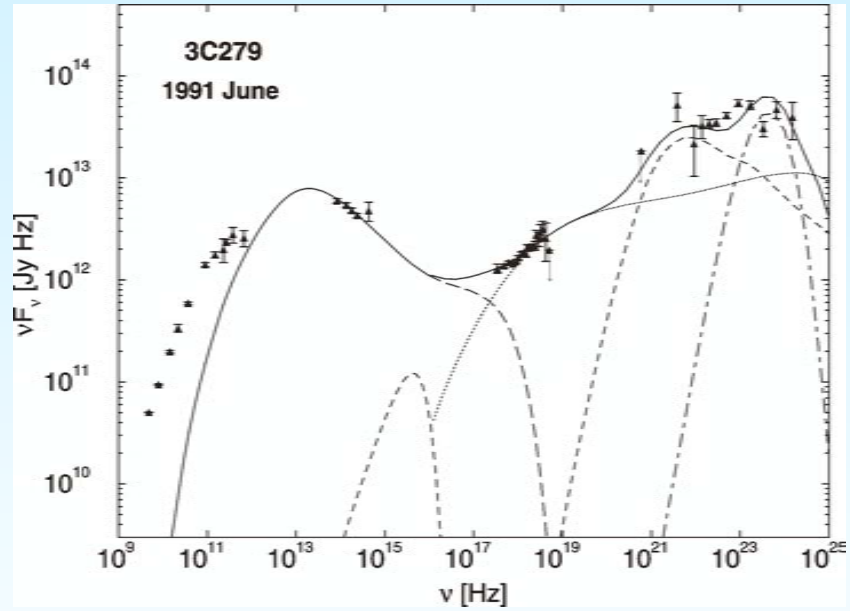

Leptonic radiation processes: parameters studies → ranges of Doppler factors and magnetic field strengths in pure SSC models

Detailed spectral variations result from multiple radiation components (e.g., PKS 0529+134; Böttcher and Collmar 1998)

Correlated variability → information on acceleration and radiation processes

Statistics of Blazars

(CD and Davis 1999)

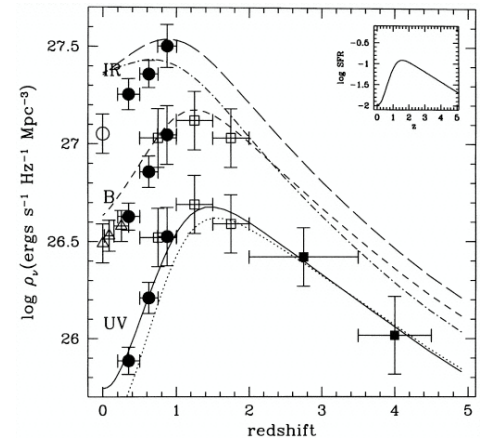

Based on model of CD and Gehrels (1995):

- randomly oriented, collimated relativistic plasma blobs
- beaming pattern given by $F \propto \delta^{4+2\alpha}$
- Comoving density of blazars proportional to star formation rate history of universe (Madau et al. 1998)

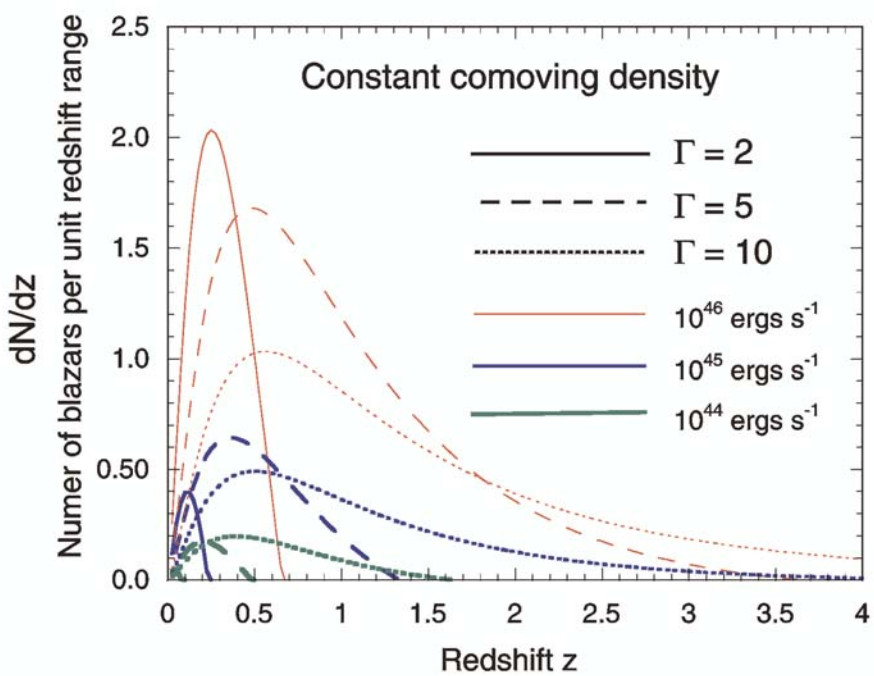

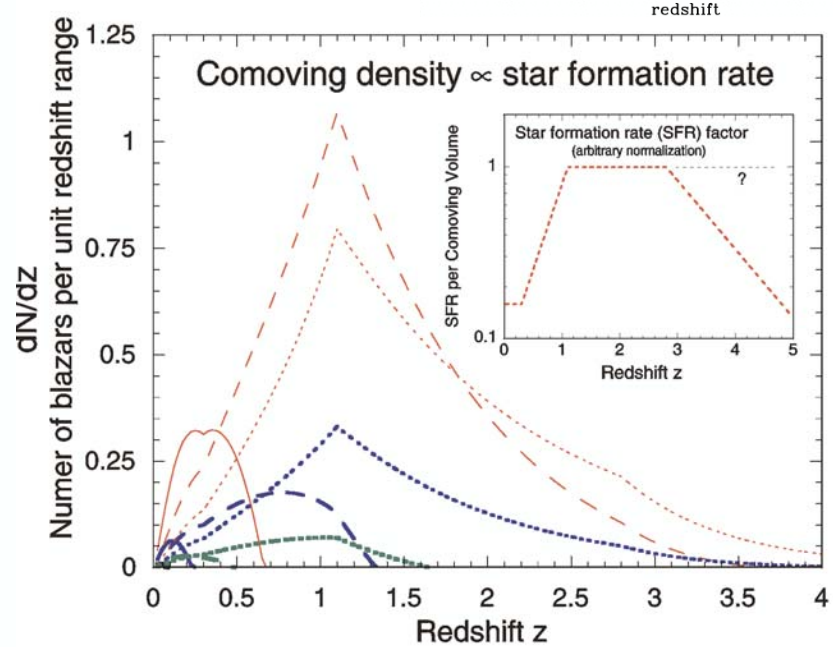

Model fitting depends only on comoving luminosity in blob and bulk Lorentz factor of blob, and assumption about source density with redshift

(approach differs from Chiang & Mukherjee (1998) by considering density rather than luminosity evolution.)

Fit to Redshift Distribution of Blazars

Redshift distributions for constant comoving density model does not give good fit to the data (especially for the FSRQs): it peaks at too small a redshift

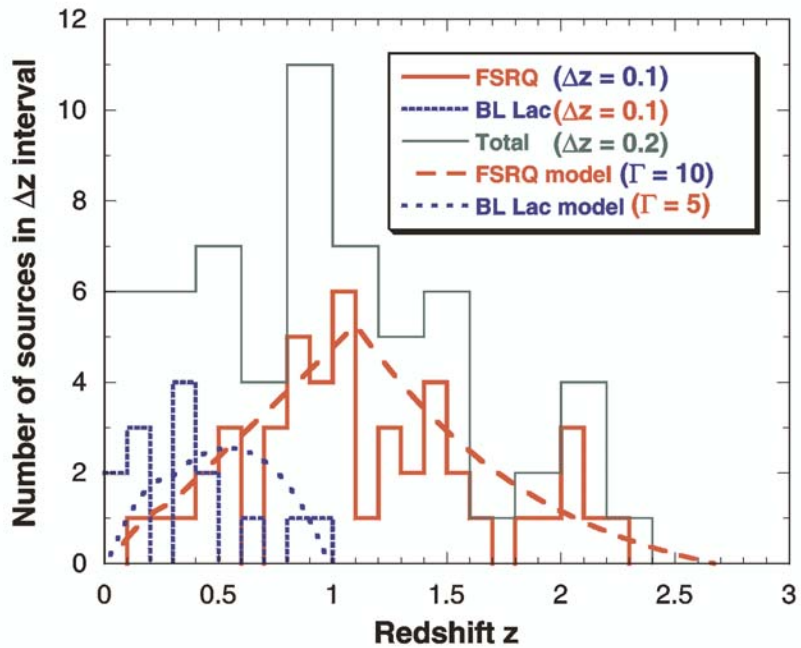

Model with blazar density proportional to SFR give a good fit to the redshift and flux distributions

Predicted Redshift and Flux Distribution Observed with GLAST

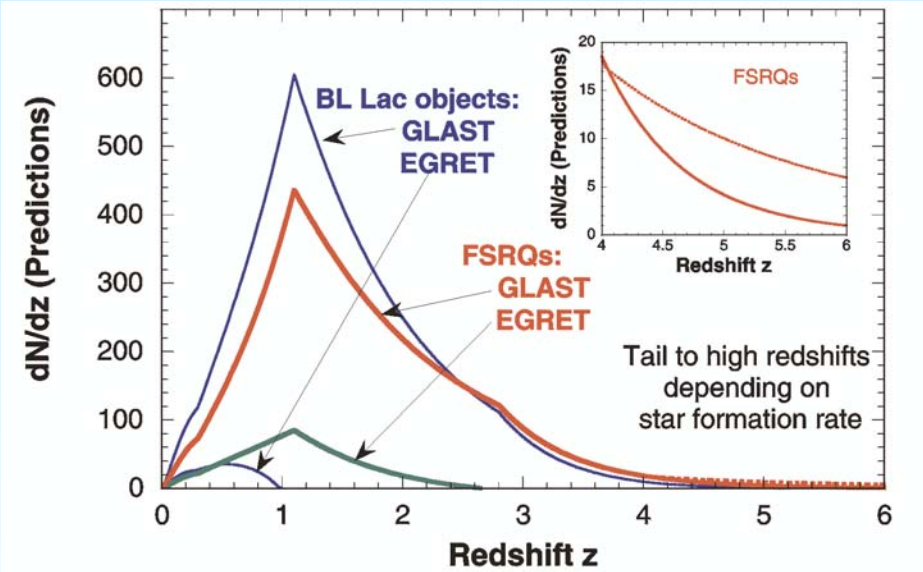

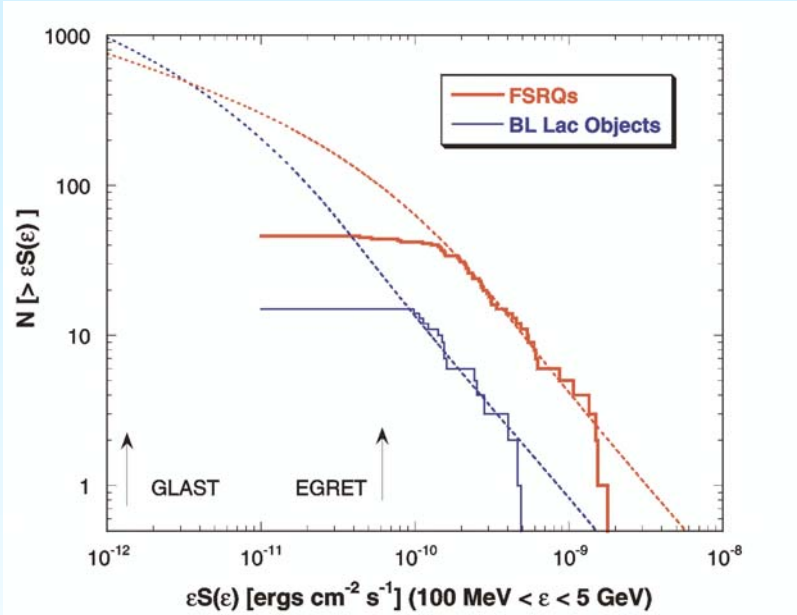

Extrapolating to the flux threshold for GLAST ⇒ GLAST should detect ~ 2000 blazars and a larger fraction (50% rather than the 25% observed with EGRET) should be BL Lac objects.

Predict a flowering of BL Lac objects with GLAST

Most will be "high-frequency peaked" BL Lac objects, many of which will not have been previously identified, and will provide a rich new class of targets for TeV observatories.

Blazars contribute large (> 30%) fraction of extragalactic gamma-ray background

The Evolution of Active Galaxies

The nuclear activity in a galaxy evolves in response to the changing environment, which itself imprints its presence on the spectral energy distribution of the galaxy.

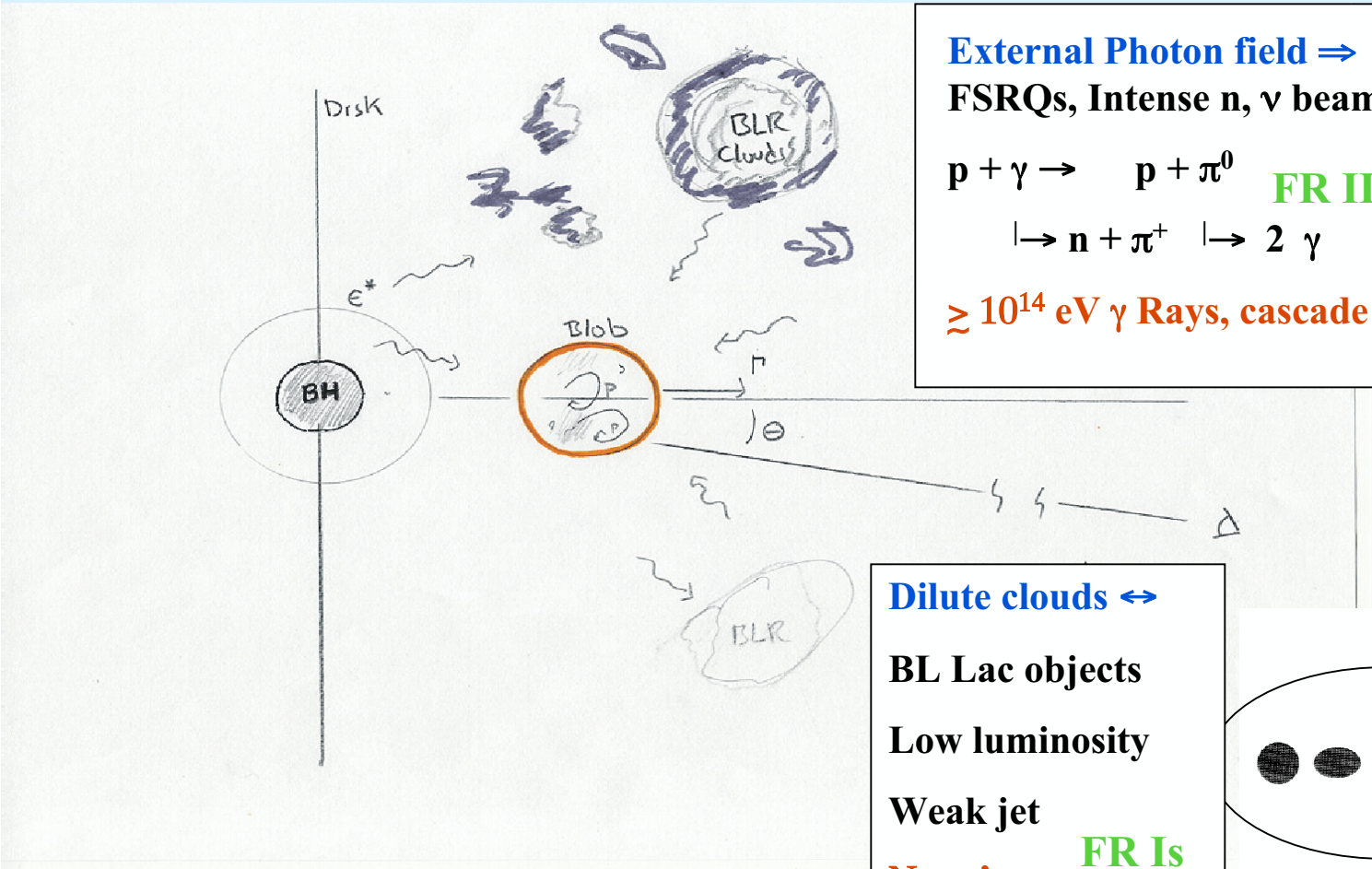

External Photon field ⇒

FSRQs, Intense n, ν beam

$p + \gamma \rightarrow \quad p + \pi^0$ **FR IIs**

$\quad \hookrightarrow n + \pi^+ \quad \hookrightarrow 2\ \gamma$

$\gtrsim 10^{14}$ eV γ Rays, cascade

Dilute clouds ↔

BL Lac objects

Low luminosity

Weak jet

No ν's **FR Is**

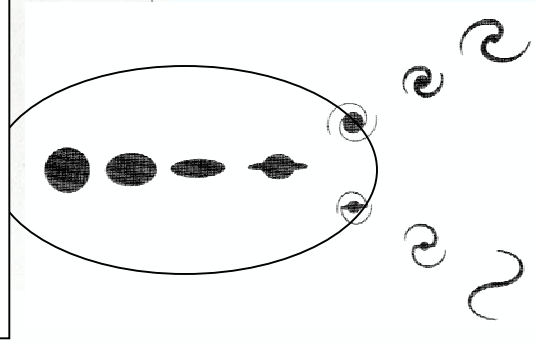

Blazar Sequence Comparison

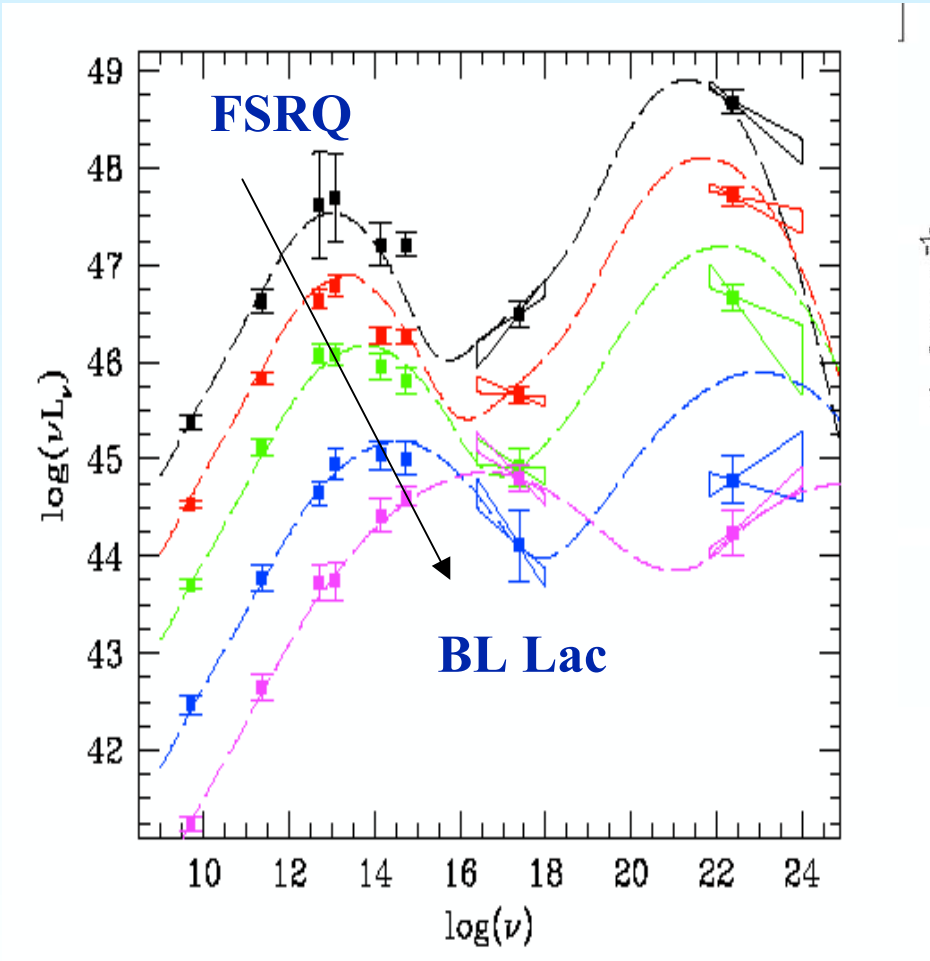

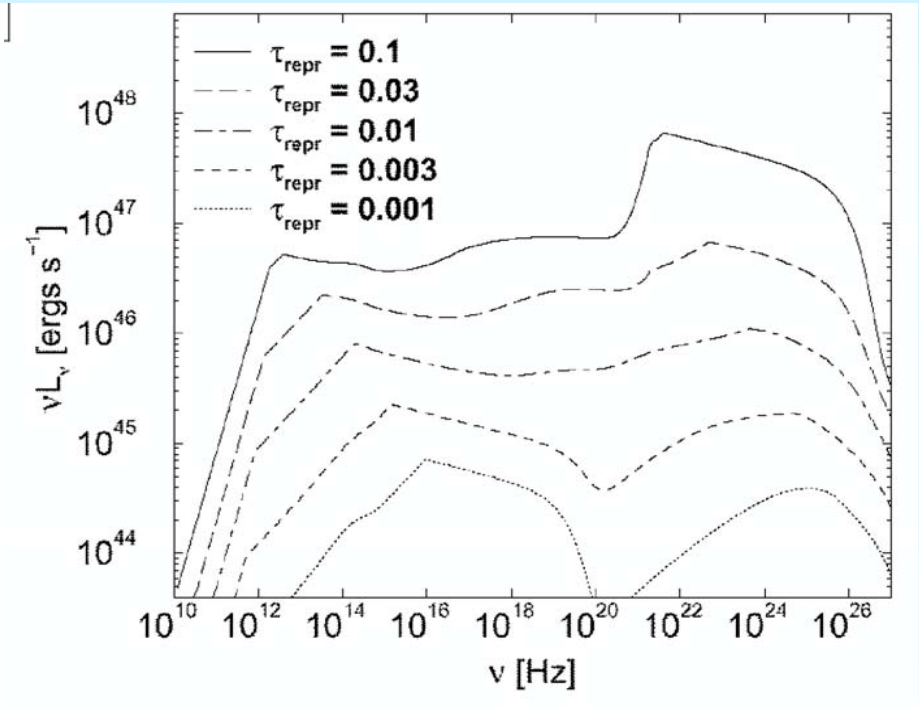

- Evolution from FSRQ to BL Lac Objects in terms of a reduction of fuel from surrounding gas and dust

Böttcher and CD (2002)

EBL

Stecker et al.
Observational SEDs;
assumed z-distribution

vs.

Primack et al.
Population Synthesis
Methods

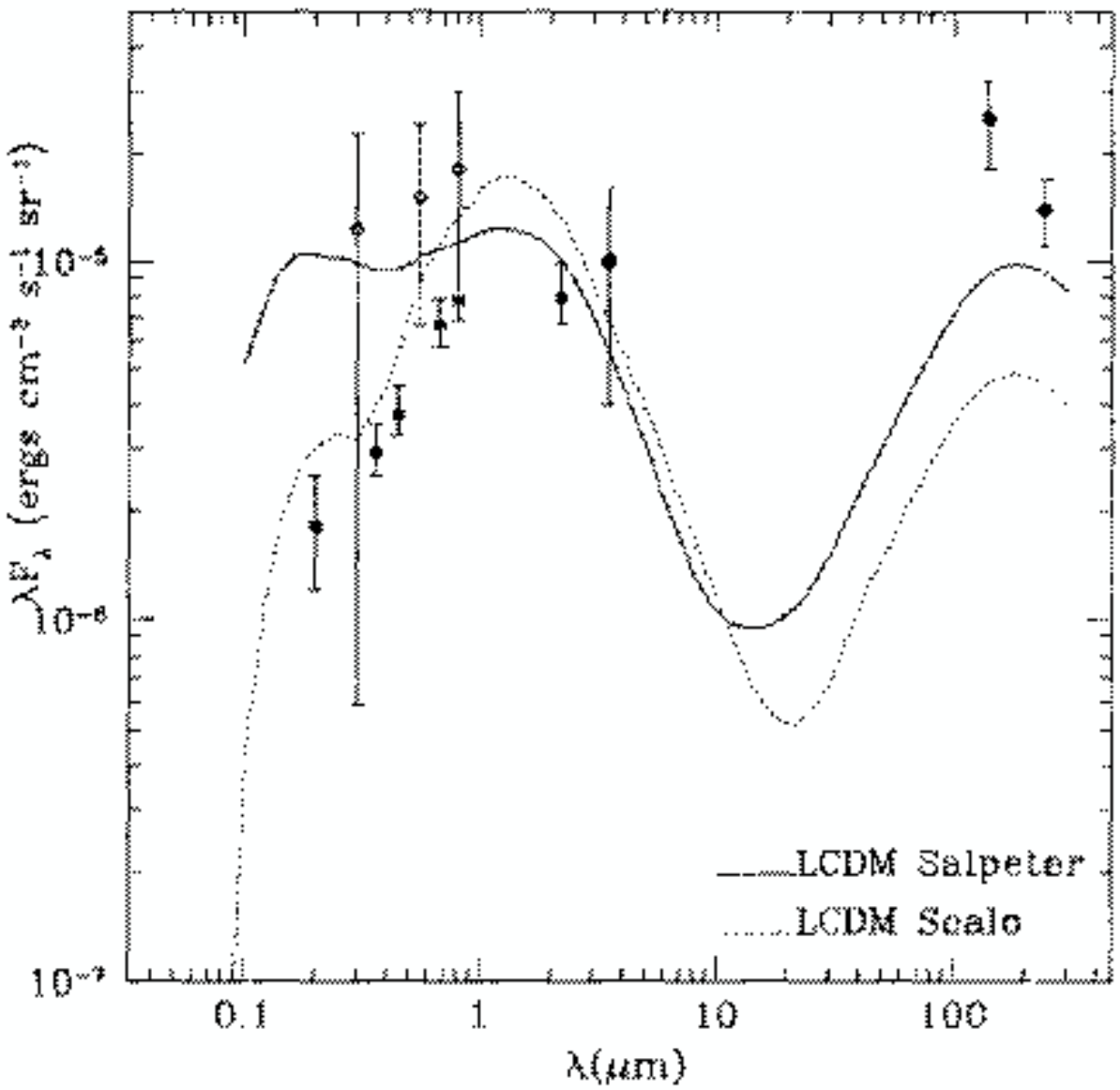

What about Nonthermal Protons and Ions?

Nonthermal particles;
Intense photon fields

Importance of external radiation field for photomeson production in FSRQs

$\Rightarrow$ Strong photomeson production

$$p + \gamma \rightarrow n + \pi^{+} \ , \ p + \pi^{0}$$

Nonthermal Proton Spectrum

$$L_p = 2\times10^{48}\delta^{-4}\ ergs\ s^{-1}$$

$$N_p(\gamma_p) \propto \gamma_p^{-2}$$

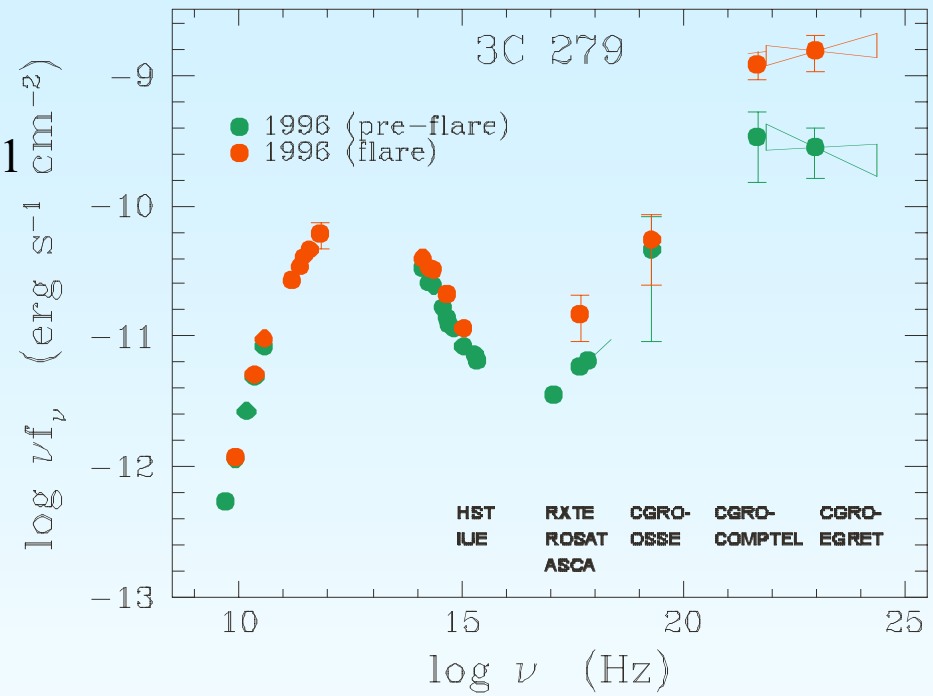

• Nonthermal proton power corresponds to average γ–ray luminosity measured from 3C 279 in 1996 based on two day flare and 3-week average spectral fluxes (Wehrle et al. 1998)

$$r_L = (3.1\times10^6 cm)\gamma_p^{max} / B(G) < r_b \Rightarrow E_p << 10^{20} Z\ eV$$

Photomeson Neutrino Production Calculations

B and δ

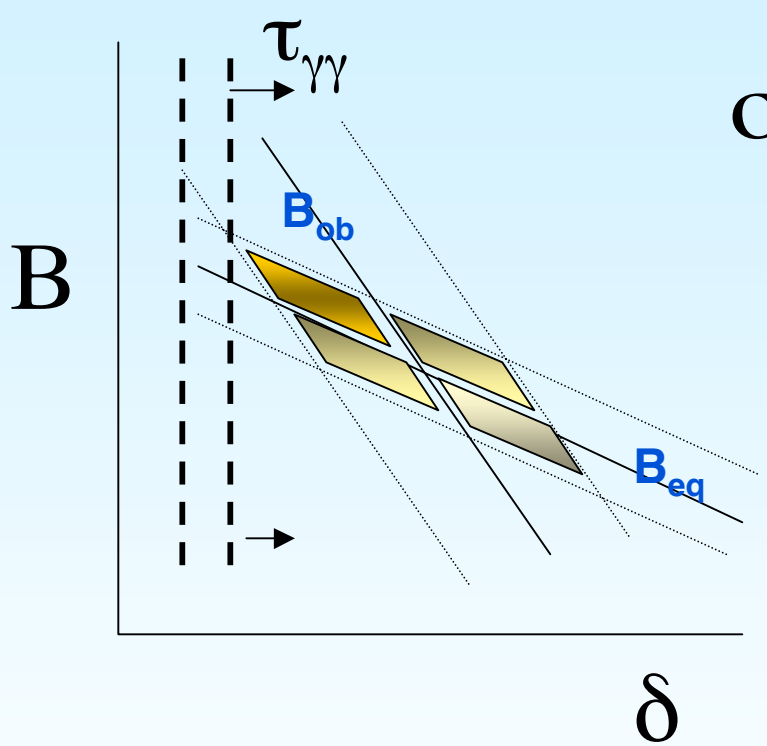

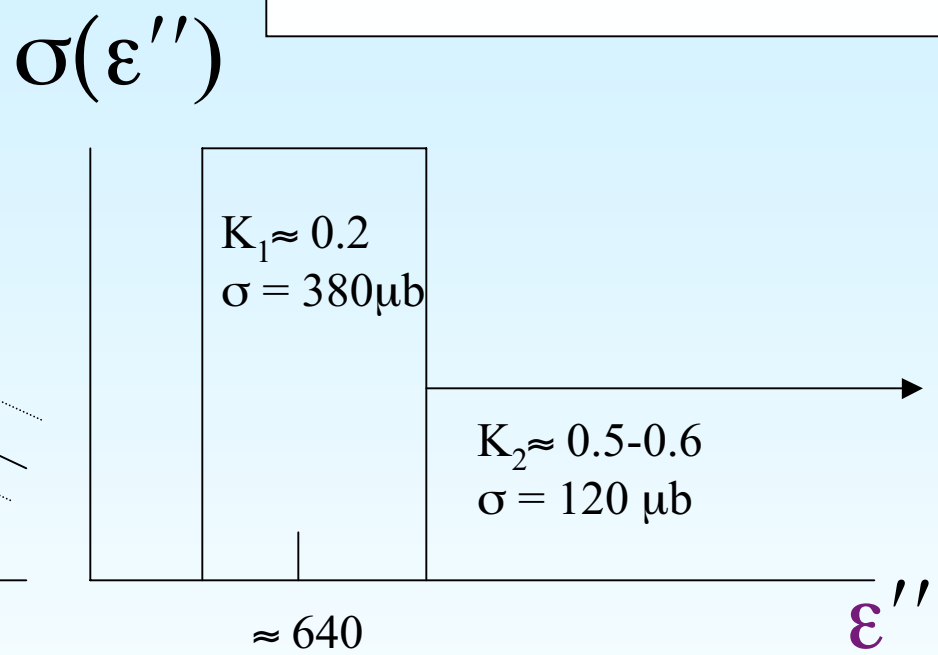

$$t_{p\gamma}^{-1}(\gamma_p) = \int_{\frac{\epsilon_{th}}{2\gamma_p}}^{\infty} d\epsilon' \, \frac{c\, n'_{ph}(\epsilon')}{2\gamma_p^2 \epsilon'^2} \int_{\epsilon_{th}}^{2\epsilon'\gamma_p} d\epsilon_r \, \sigma(\epsilon_r) K_{p\gamma}(\epsilon_r) \epsilon_r \ ,$$

Photomeson Production Energy-Loss Timescales

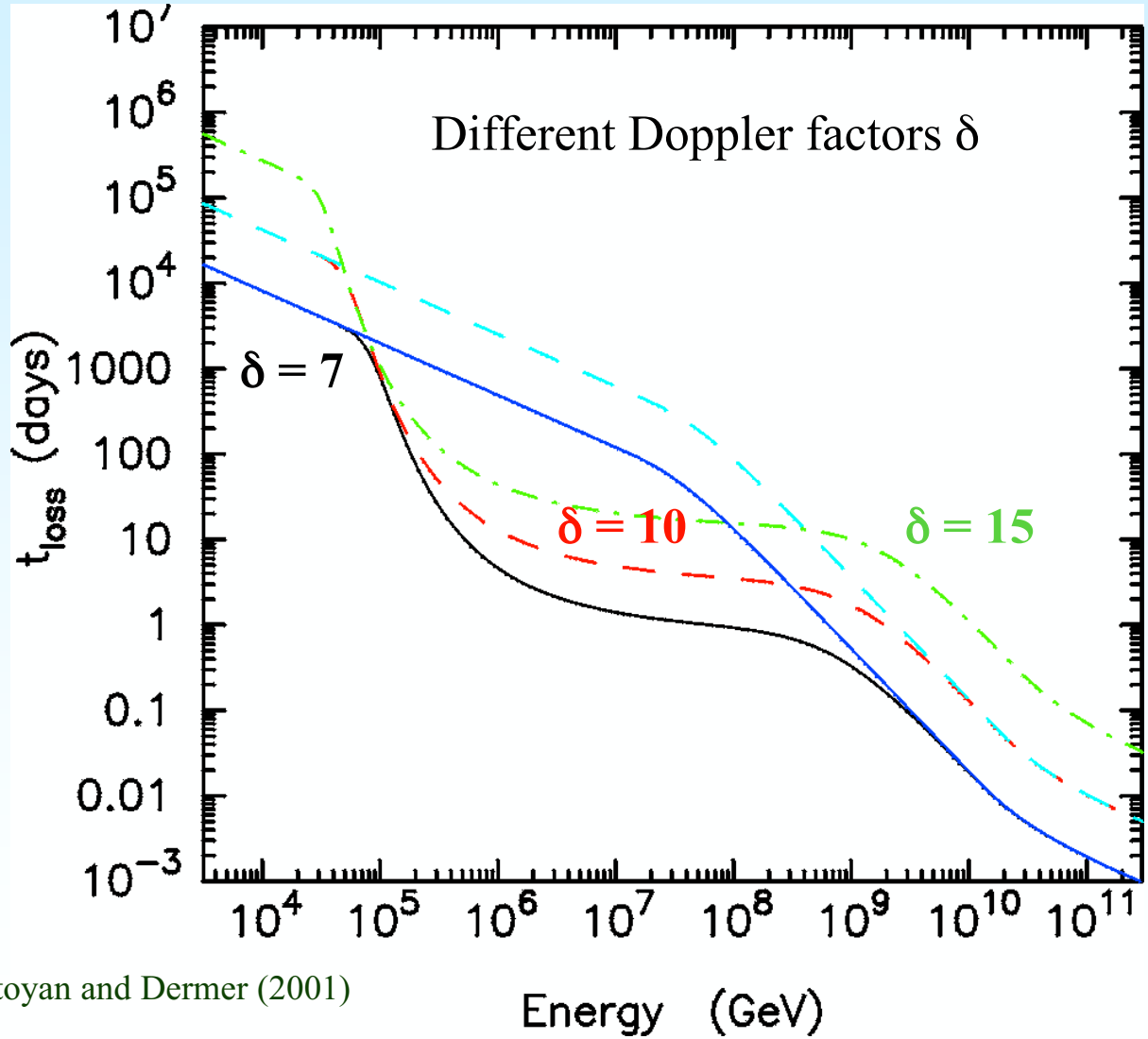

Atoyan and Dermer (2001)

- timescales in observer frame for properties derived from 3-week average spectral fluxes from 3C 279 in 1996 (Wehrle et al. 1998)
- t_{var} = 1 day
- compare case with no external field
- impact of UV field: ***higher fluxes and lower energies of ν ⇒***

Much larger numbers of ν to detect

Energy Distributions of Relativistic Protons

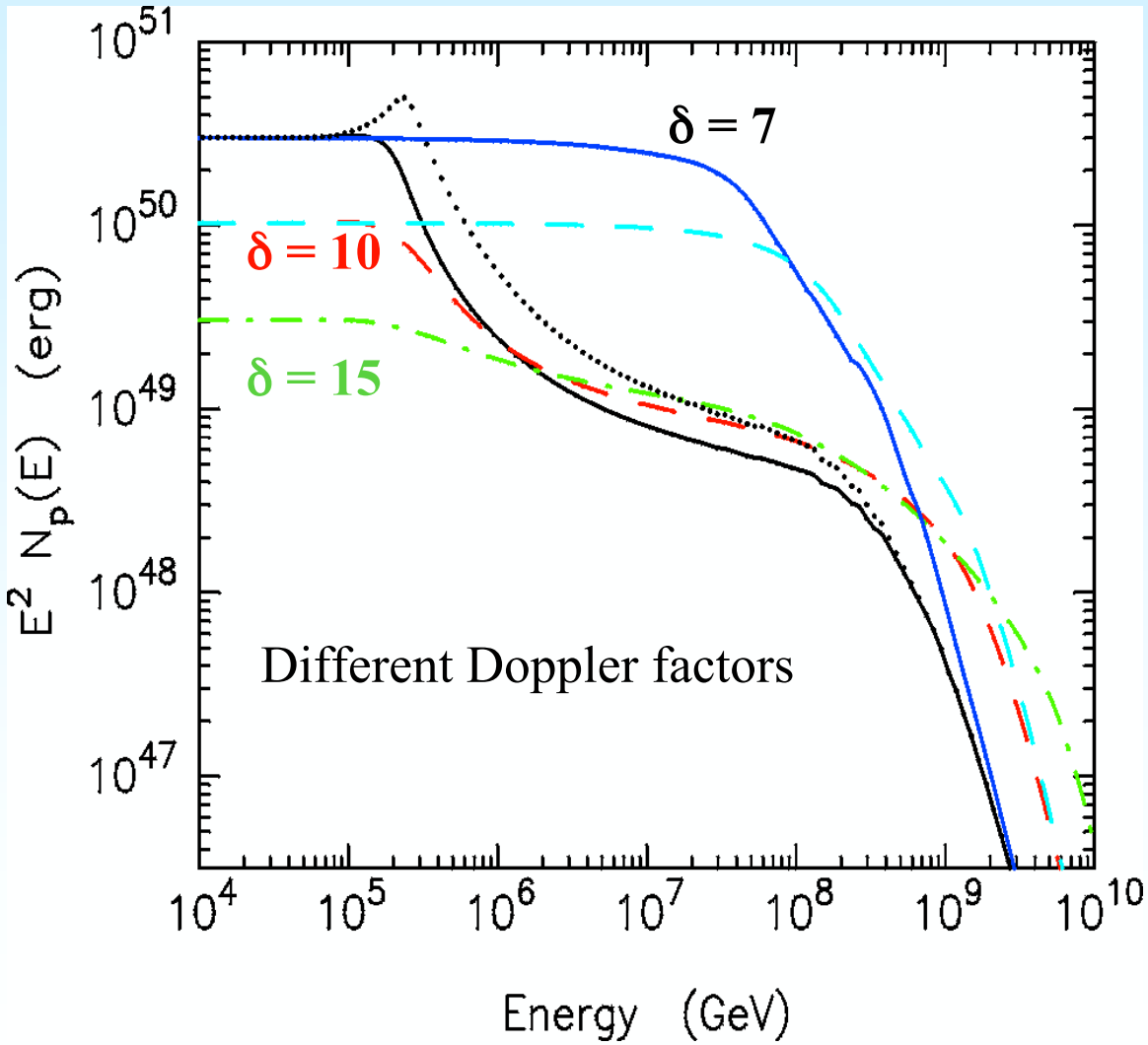

Proton distribution after 3 weeks, with and without external field (parameters for 3C 279 with 3 week average flux)

Dots: no neutron escape

$$p + \gamma \rightarrow n + \pi^+$$

Nonthermal proton accumulation

Energy Distributions of Relativistic Protons

Different blob parameters

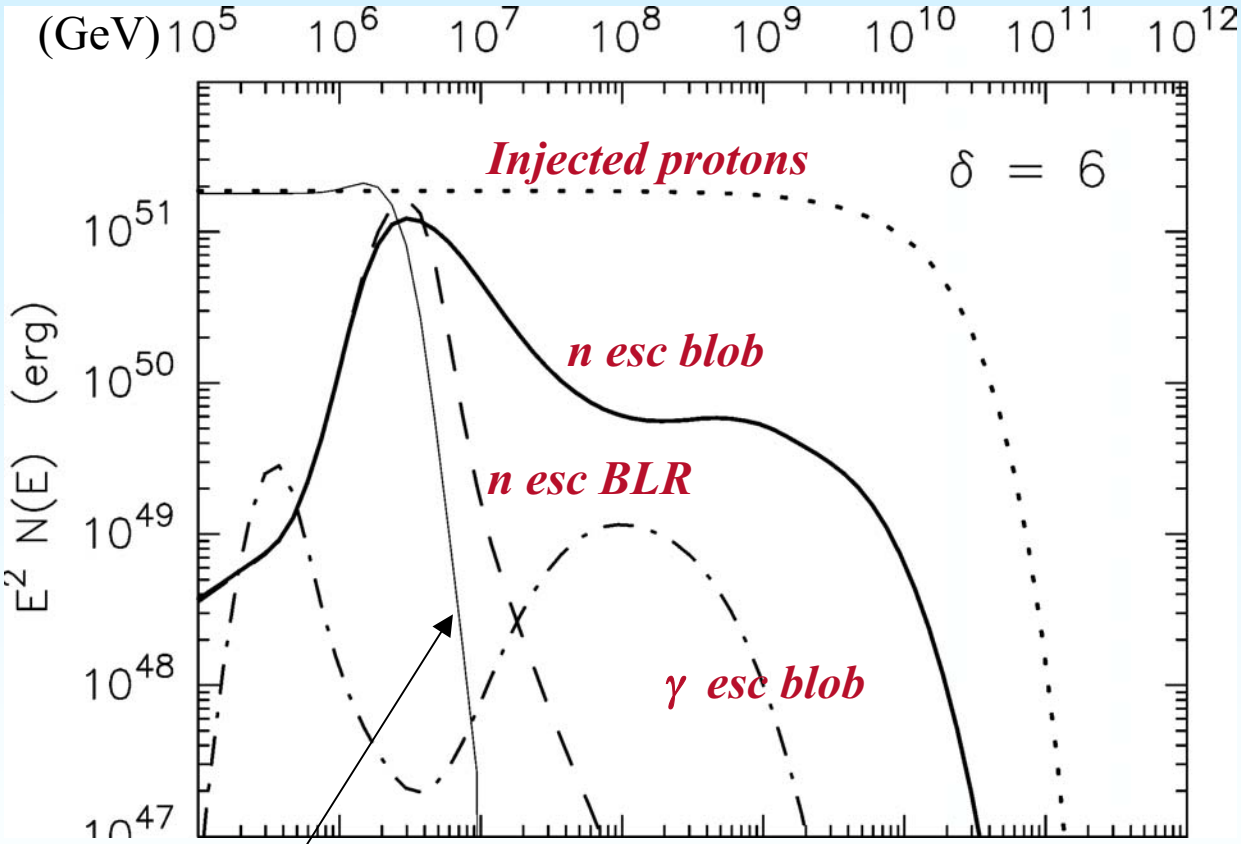

proton distribution when blob leaves BLR

Proton distribution after 3 weeks, with and without external field (parameters for 3C 279 for 2 day flaring behavior)

High-energy (> 10^{14} eV) gamma rays cannot escape the blob directly due to γγ attenuation on the internal radiation field

Neutrino/γ-Ray Fluences from 3C 279 ('FRII blazar')

Different Doppler factors

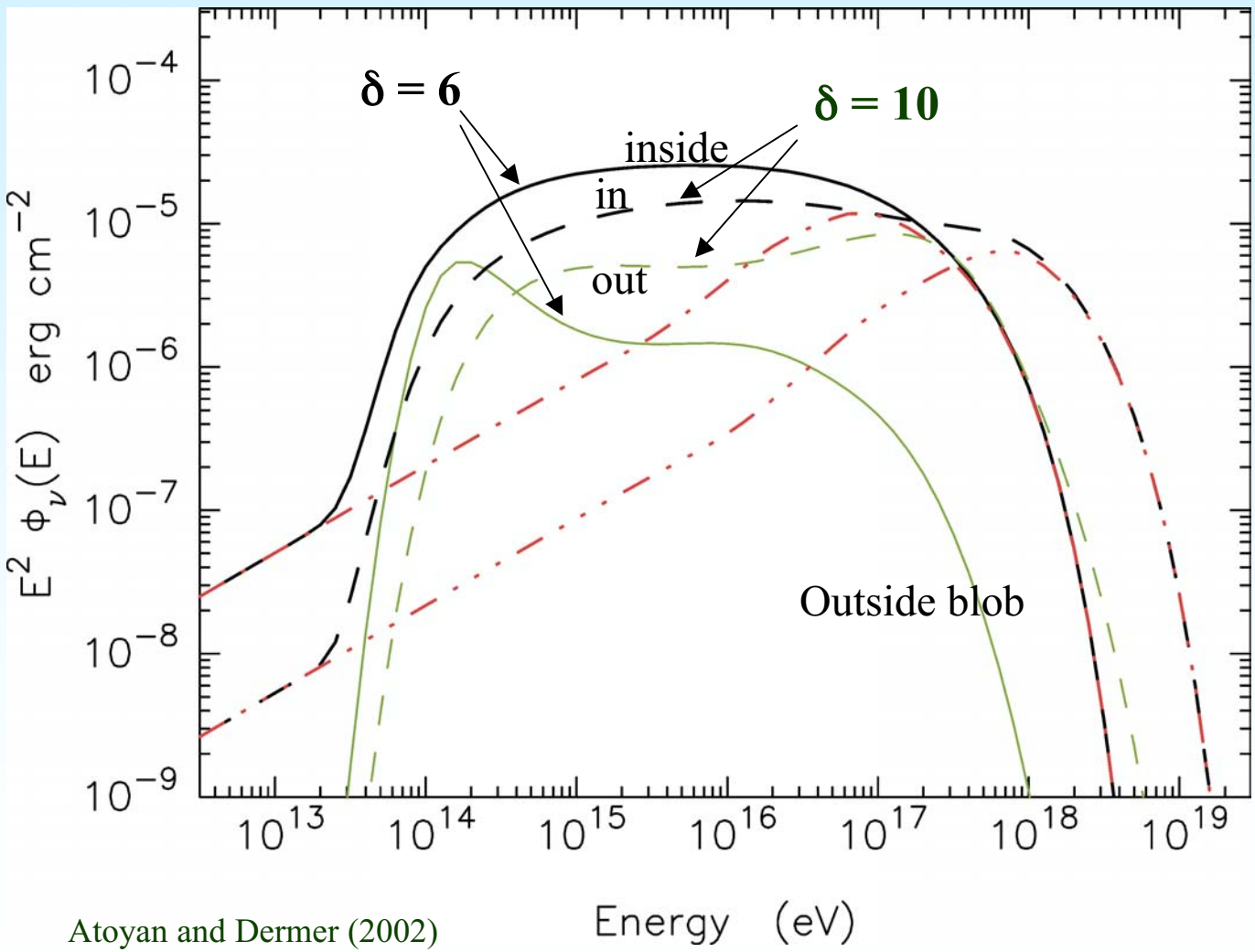

Atoyan and Dermer (2002)

Δt = 2 d (Feb. 14-16, 1996)

N_ν expected by IceCube:

$N_\nu \approx 0.33$ for $\delta = 6$,

and

$N_\nu \approx 0.2$ for $\delta = 10$

Without pγ on UV:

$N_\nu \approx 0.026$ for $\delta = 6$ (dot-dashed)

$N_\nu \approx 0.005$ for $\delta = 10$ (3-dot-dashed)

Neutrino Fluences from Mrk 501 ('FRI blazar')

(Different Doppler factors)

from Mrk 501 ('*BL Lac object*')

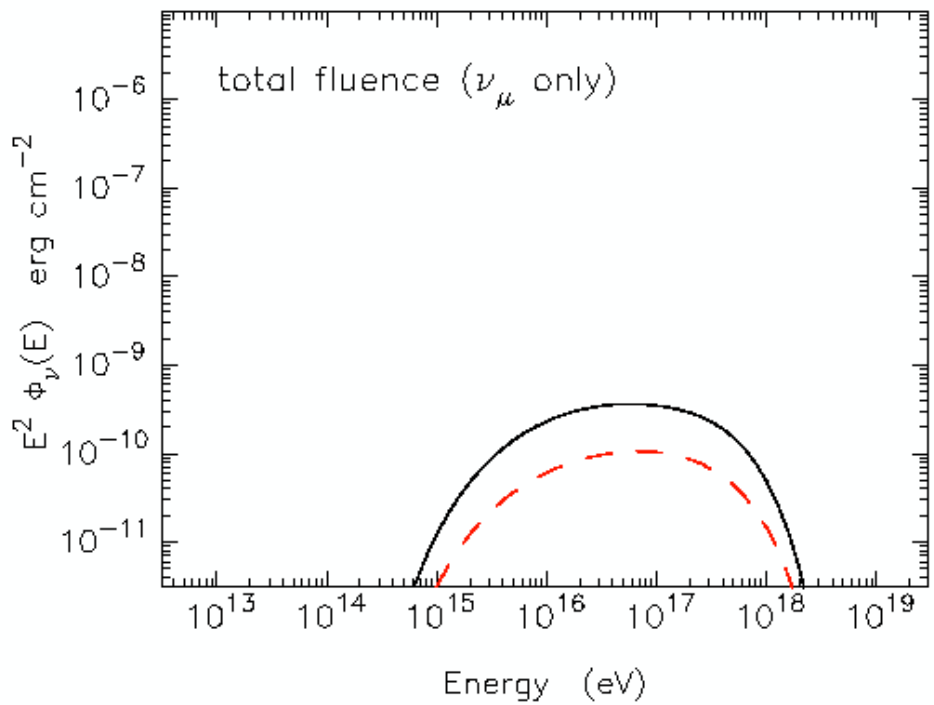

$\Delta t = 1\,\mathrm{d}$ (April 16, 1997), $B = B_{eq}$

$N_{\nu_\mu} \approx 5.7 \times 10^{-6}$ for $\delta = 10$ (*solid*), and $N_{\nu_\mu} \approx 1.5 \times 10^{-6}$ for $\delta = 25$ (*dashed*);

Neutrinos from AGN: expected or not?

Powerful FSRQ/ FRII blazars: Yes

- $(0.2 - 0.3)\ \nu$ per flare $[\ \dot{E}_{prot}(accel.) = L_\gamma(observed)]$

$\Longrightarrow$ $\underline{N_\nu \simeq 2 - 3}$ for ~ 10 flares (during 1-3 yrs)

and/or during a single event [if $\dot{E}_{prot}(accel.) \sim 10 \times E_{electr}(accel$

- N_ν <u>in low state</u> :

$(persistent\ !)$ γ-level of 3C 279 $\sim 0.1\, F_\gamma(flare)$ (EGRET)

$\Longrightarrow$ if $\dot{E}_{prot}(low) \sim \dot{E}_{electr}(low)$
(and since UV photon target is always there!)

$$N_\nu \sim 4 - 6\, \nu_\mu/\mathrm{yr} \text{ in low state}$$

- BACKGROUND (ATMOSPHERIC) ν_μ:

$$N_\nu(> E) \simeq 0.14 \left(\frac{E}{10\,\mathrm{TeV}}\right)^{-1.7} \left(\frac{\Omega}{1\,\mathrm{deg}^2}\right) \frac{S_{det}\Delta t_{obs}}{1\,\mathrm{km}^2\,\mathrm{yr}}$$

$\Longrightarrow$ **even $N_\nu \geq 2$ at $E \geq 30\,\mathrm{TeV}$ will be a significant detection of an AGN !**

ν / UHECR source Indicators: *Large-Scale X-ray Jets*

NEUTRAL UHE PARTICLE BEAMS

(UHE neutrons & γ-rays)

emerging from the inner jet:

take away $\sim 10\%$ of all $W_{CR}(> 1\mathrm{PeV})$

(by neutrons with $E_n \geq 10^{17}$ eV; and γ-rays with $E_\gamma > 10^{15}$ eV)

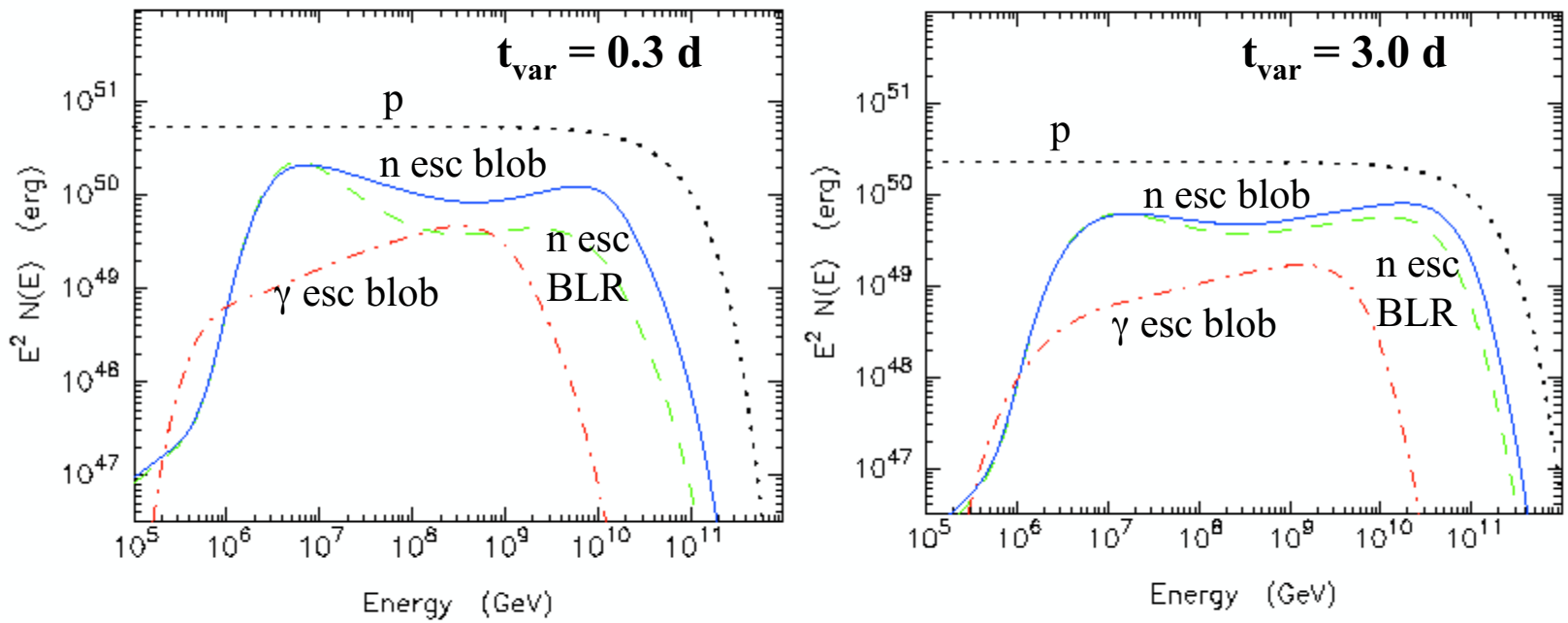

solid: neutrons escaping the inner jet (at $R \leq 1$ pc)

dashed: neutrons escaping external UV-field region

dot-dashed: γ-rays escaping external UV-field region

dotted: protons injected in the compact jet

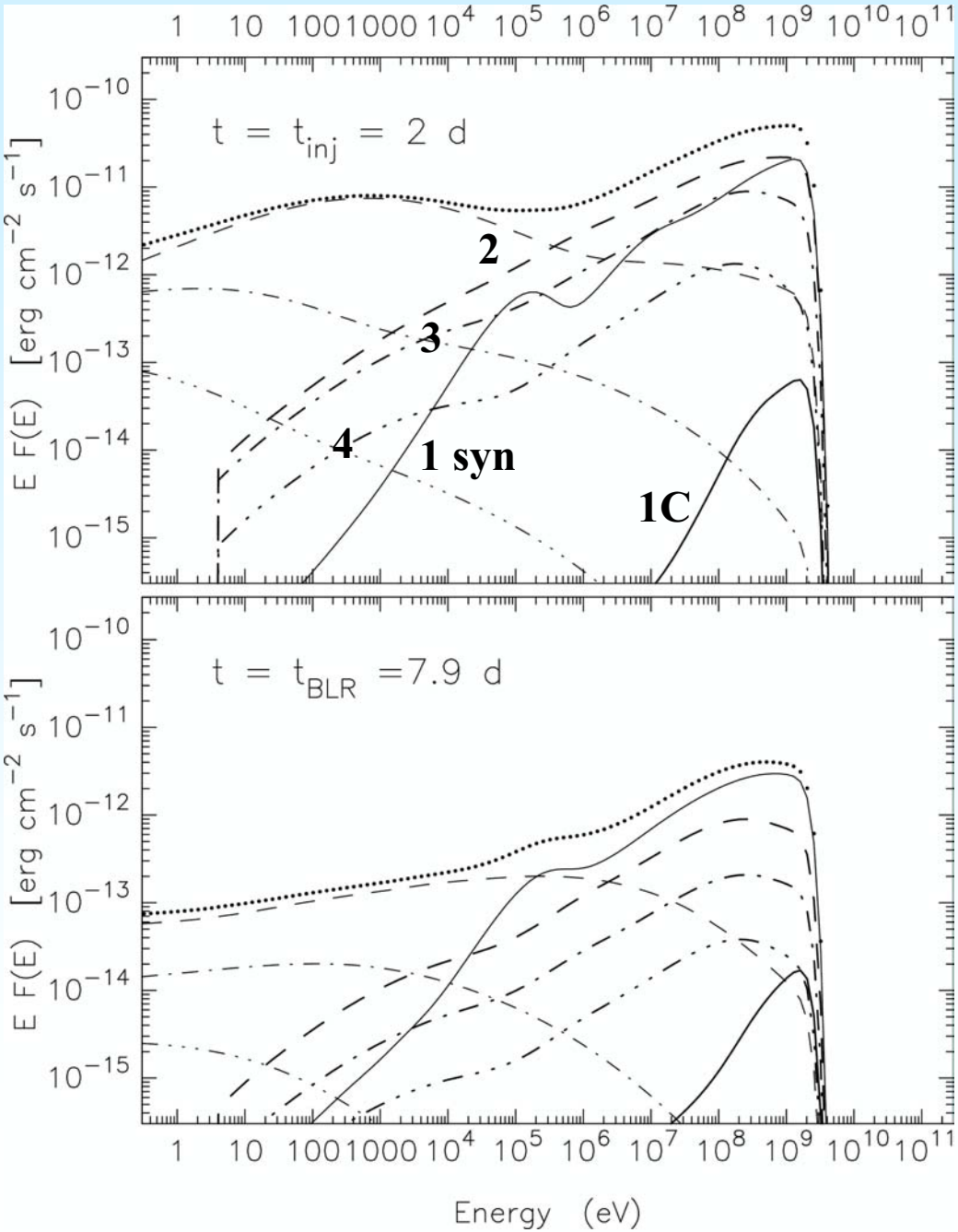

Hadronic Cascade Radiation for 3C 279

- Limits proton/electron injection ratio
- Inverse correlation between cutoff energy and neutrino production efficiency

Observational Evidence for Sites of UHECR Acceleration

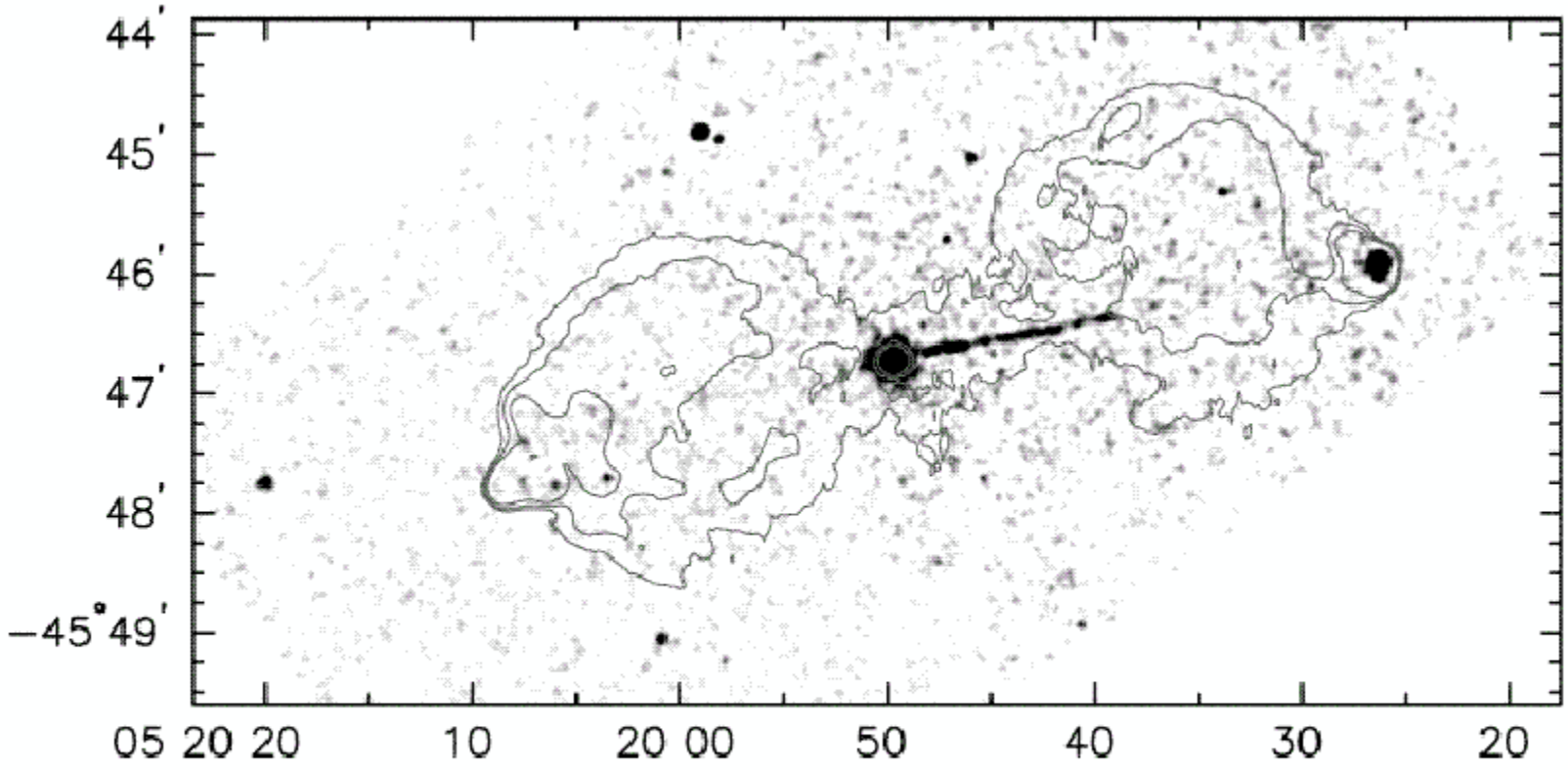

> 100 kps scale jet of Pictor A (Wilson et al. 2001, ApJ 547, 740)

Powering the Extended Jet

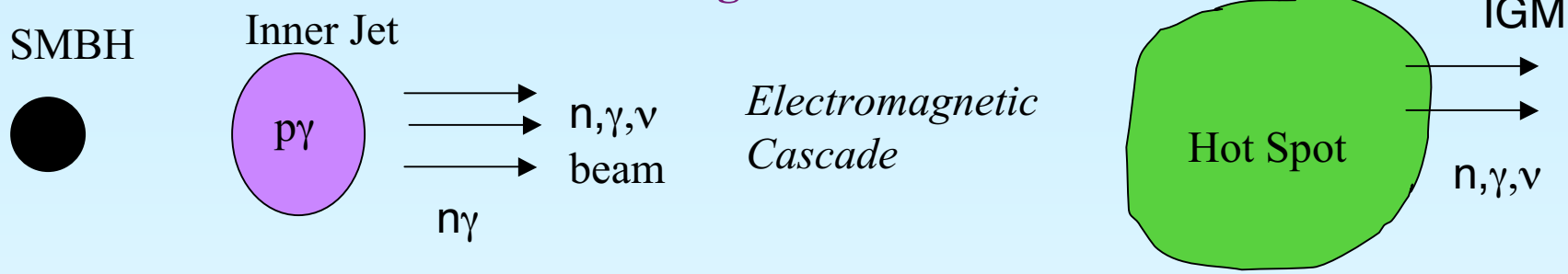

- **Ultra-high energy photons made by nγ production in Broad Line Region outside blob**
- **Photons with energies > 100 TeV are attenuated by CMB and DIIRF background**
- **Neutrons decay at $E_n/(10^{17}$ eV) kpc**
- **Avoids jet quenching problem**
- **Difference between FR I and FR II galaxies**
- **Beam energy powers lobes and hot spots in extended jet**
- **Gamma Ray Halos to be detected with GLAST**

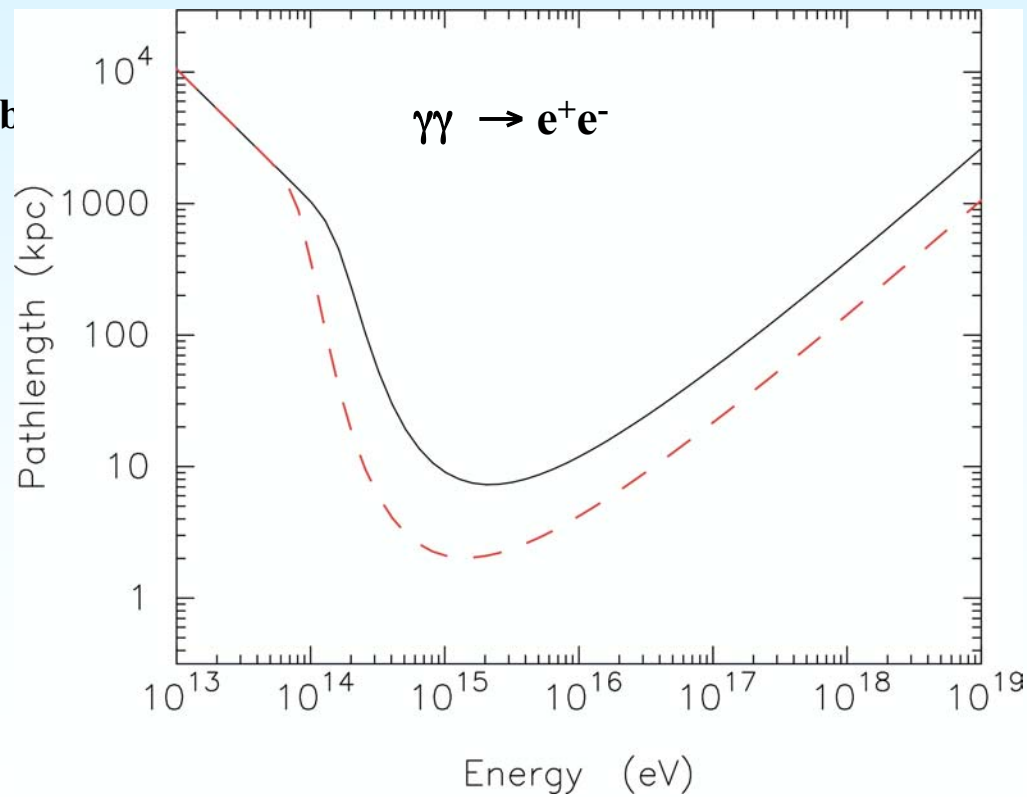

X-rays from the Extended Jet

Sambruna et al. 2001

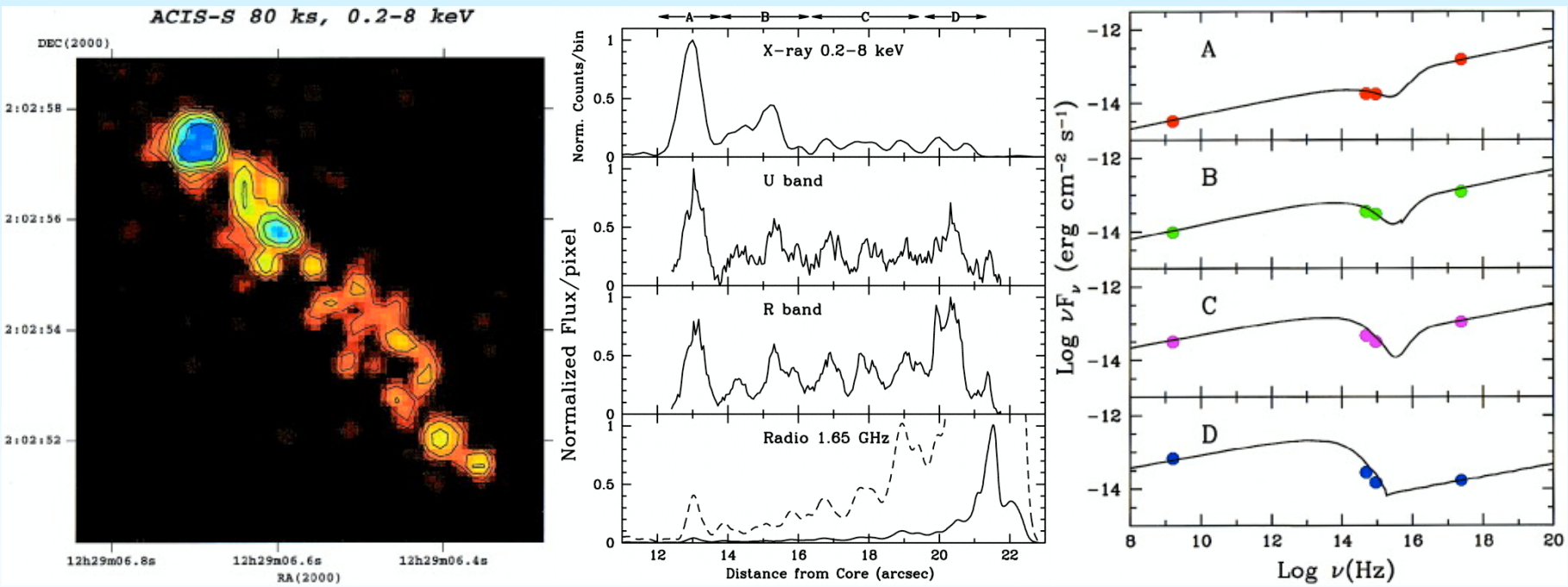

3C 273

X-ray emission from extended jet:

- **SSC**
- **Compton-scattered CMB**
- **synchrotron**

Synchrotron Model for Extended Chandra X-ray Jets

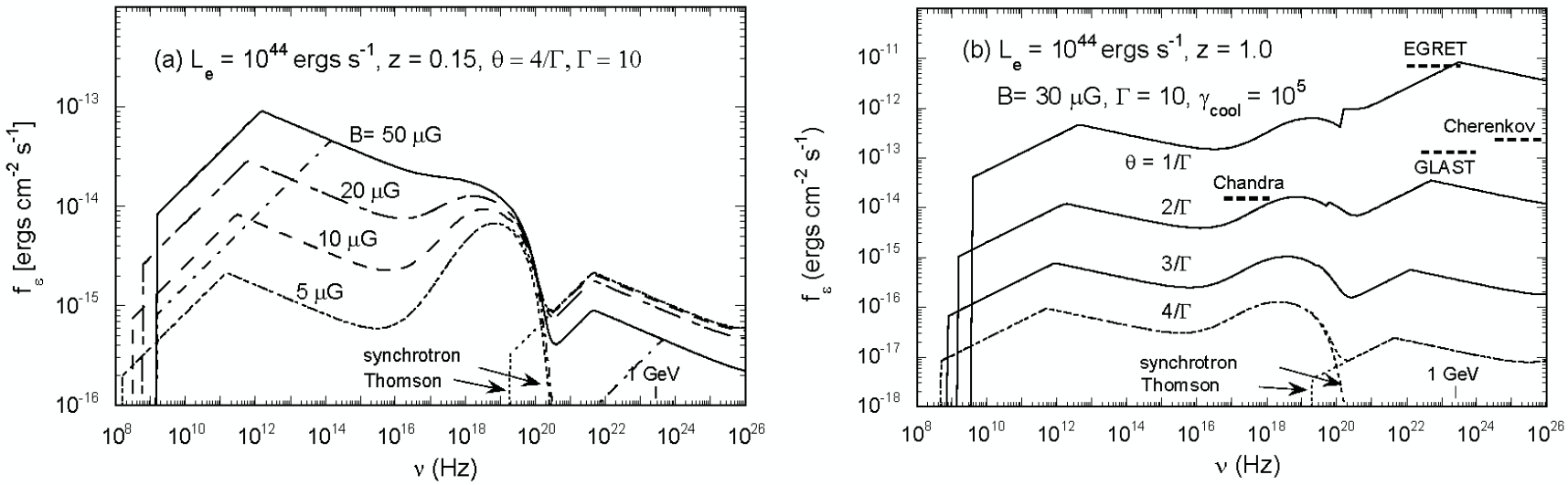

CD and Atoyan (2002)

Combined Compton and Synchrotron Losses

Klein-Nishina decline on electrons with $\gamma > 2\times10^8/\Gamma(1+z)$

X-ray synchrotron spectral hardening at

$$\nu > 8\times10^{16} B_{\mu G}/[\Gamma^2(1+z)^3]\ Hz$$

Active Galaxy Evolution

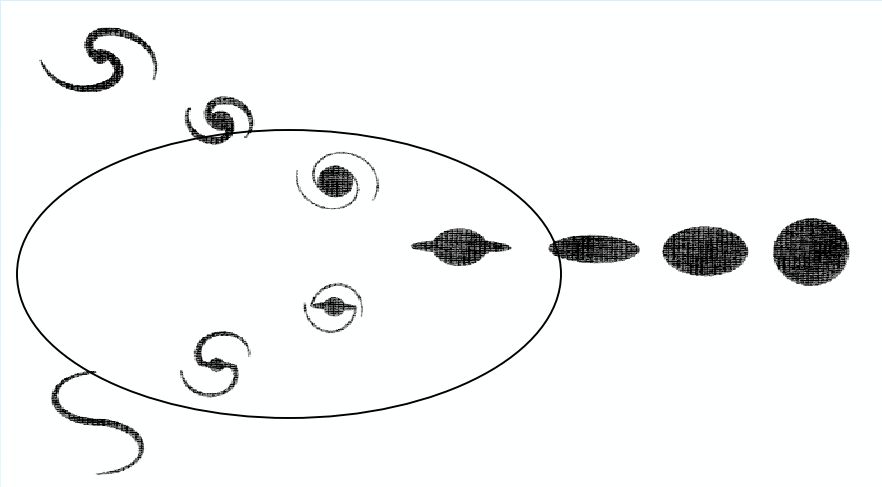

- Dark matter halos collapse from initial spectrum of density fluctuations
  - Press-Schechter formalism for collapse on different mass scales
  - Hierarchical structure formation (bottom-up)
- Infrared luminous galaxies: Buried ν sources
- Black Hole Jet formation
- Galaxy mergers and fueling: evolution of active galaxies
- Formation of jets in FR II and FRI radio galaxies by neutral beams
- Extended X-ray emission from jet sources
- Neutrino and γ-ray test of active galaxy evolutionary scenario

Active Galactic Nuclei Evolutionary Scenario

will be tested by and GLAST

(γ-ray halos around FR II galaxies, but not around FR I galaxies; Statistics of BL Lacs and FSRQs)

And

Neutrino Telescopes

(Neutrinos from FSRQs rather than BL Lacs; buried neutrino sources in Infrared Luminous Galaxies)

GLAST Strategies

1. Time Series Analysis of Blazar Data
   Periodic/QPO

2. Time Correlation Studies
   Cross Frequency/Long Baseline

3. Subtraction of Variable Background
   Upper limits to nonvariable components

4. Occultation analysis
   Angular Resolution Enhancement